Resource Allocation for URLLC Service in In-Band Full-Duplex-Based V2I Networks

Chun-Hao Fang, *Student Member, IEEE*, Kai-Ten Feng, *Senior Member, IEEE*, and Lie-Liang Yang, *Fellow, IEEE*

Abstract— This paper investigates the first resource management problem for vehicular-to-infrastructure (V2I) networks under the in-band full-duplex (IBFD) backhauling scheme with guaranteed ultra-reliable and low-latency (URLLC) service. The considered networks suffers from interference caused by three node transmission in IBFD scheme and the mobility of vehicular user equipments (VUEs). The resource allocation problem is formulated to jointly optimize VUE association, resource block assignment (RA) and power allocation (PA), while satisfying the reliability and latency constraints at the same time. The formulated problem is a mixed integer non-linear problem with non-convex objective function and constraints. Finding globally optimal solution for this type of problem is still an open problem. To develop tractable solutions, the original problem is firstly simplified using derived equivalent expression for the objective function. The proposed method then decomposed it into RA and PA sub-problems. In each iteration, the PA sub-problem is solved for a set of given PA solution; while the solution for PA sub-problem is searched under determined RA results. The RA and PA sub-problems are solved iteratively until the converging condition is achieved. Theoretical analysis proves that the proposed method achieves Nash-stable equilibrium and local optimality for RA and PA sub-problems respectively. Simulation results verify the effectiveness of the derived performance analysis and demonstrate that the proposed algorithm outperforms the state-of-the-art algorithms in the literatures.

Index Terms— In-band full-duplex, self-backhaul, vehicle-to-infrastructure networks, Doppler shift, handover delay, ultra-reliable and low-latency communications, matching game, coalition game.

I. Introduction

IN RECENT years, the increasing number of traffic congestion gives rise to the evolution of transportation systems.

Chun-Hao Fang and Kai-Ten Feng are with the Department of Electrical and Computer Engineering, National Yang Ming Chiao Tung University, Hsinchu 300, Taiwan (e-mail: eie5577.cm03g@nctu.edu.tw; ktfeng@nycu.edu.tw).

Lie-Liang Yang is with the School of Electronics and Computer Science, University of Southampton, Southampton SO17 1BJ, U.K. (e-mail: lly@ecs.soton.ac.uk).

In the meantime, the global market of self-driving cars are estimated to reach 20 billion by 2024 due to demand for on-wheel infotainment, which lead to accelerated interest in vehicular communications for automotive industry [1]. As autonomous vehicles are rapidly developed, vehicle-to-everything (V2X) communications are emerging as a promising technology to provide traffic efficiency in the fifth-generation (5G) wireless networks [2]. Since self-driving vehicles have to collect critical information timely in the fast changing network topology [3], performance of V2X is greatly dependent on ultra-reliable and low-latency communications (URLLC) and several literatures have investigated various design aspects [4]–[8]. [4] develops a beamforming design for downlink (DL) URLLC systems in the short block length regime, which generates a sequence of improved feasible points and converges to a local optimum. [5] further considers a joint beamforming design and power allocation problem for DL URLLC systems with short packet transmission. By leveraging insights from achievable rate function, the method outperforms zero-forcing beamforming with water filling allocation. [6] studies joint power and resource allocation for URLLC vehicular networks. A novel distributed approach based on federated learning is proposed, which obtains the performance that is close to a centralized solution with up to 79 % reductions in the amount of exchanged data. To consider the influence of channel state information (CSI) variation, [7] utilizes Markov decision process framework to address the problem of dynamic channel allocation by proposing a low-complexity algorithm with consideration of low latency constraint. The proposed method can achieve more than 80 % of the optimal solution with substantial computational complexity reduction. In [8], by developing a robust learning-based approach to learn the uncertainties of channel coefficient, a significant improvement is achieved for power allocation problem to provide enhanced performance for URLLC service in V2X communications. Different from works in the above literatures, resource management problem for vehicle-to-infrastructure (V2I) networks is intractable owing to that it has to simultaneously maximize total network throughput and satisfy URLLC constraint to maintain the quality of each V2I link [9]. Hence, investigating the resource allocation algorithm design for V2I networks is important for developing V2X or URLLC systems.

On account of the advantages of low cost and fast deployment, it is required to improve network capacity by decreasing the number of served users per base stations (BS). The ultra-dense small cell network (SCN) has been regarded as one of the key solutions to achieve the performance goals

in the 5G cellular networks [10]. However, the high-speed movement of vehicular user equipments (VUEs) in the V2I networks causes high handover rate and large amount of control overhead on backhaul links in the densified SCN. Consequently, performance of V2I networks can be degraded by VUEs' mobility. Specifically, the amount of data transmission is reduced by the control overhead from handover delay. In the extreme case, the service requirement of VUEs cannot be supported by small cell BSs (SBSs) if the cell dwell time is less than the handover delay when the speeds of VUEs are too large [11], [12]. Typically, VUEs' data are exchanged among multiple SBSs with fixed cable and fiber-optics over the standardized X2 interface, which is not a practically and economically viable option for 5G networks. The reason is that the application scenarios for wired backhaul links are in general established at hard-to-reach locations, e.g., lamp posts, roof tops, whereas massive implementation of wired backhaul connectivity in the densified SCN will cause prohibitively high capital expenditures and operating expense [13], [14].

It is desirable to place SBSs wherever they are needed, not where wired backhaul is available. Therefore, in-band full-duplex (IBFD) backhauling, which is also known as FD self-backhaul, is considered as an attractive alternative and enabler for low-latency communications by its properties to improve reachability and coverage, to facilitate connectivity between SBSs, and to operate transmit and receive function under FD scheme. Frequency reuse of backhaul links and access links also makes IBFD possess the benefit of simplifying hardware complexity because same hardware scheme can be adopted by both backhaul links and access links [15]. The major challenge of IBFD comes from the self-interference (SI) power [16] from transmit antennas to receive antennas of SBSs and backhaul interference from backhaul links to access links. For this reason, it is required to investigate elegant resource allocation algorithms needs to fully exploit potential benefits of IBFD systems.

Resource allocation problem for SCN with FD self-backhauls with the concept of network virtualization is formulated in [15]. To avoid the influence of signaling overhead of centralized scheme, the problem in [15] is solved by their proposed alternating direction method. To compare the performance of the IBFD and out-of band FD (OBFD) backhauling schemes, [13] indicates that performance of the IBFD backhauling strongly depends on SI power after designing hybrid backhauling spectrum allocation method. In addition to spectrum allocation, [14] investigates precoding design to maximize the weighted sum rate in heterogeneous networks. By applying the successive convex approximation technique, the algorithm in [14] is shown to be able to achieve balance among received signal and SI. Nonetheless, the designs in [13]–[15] did not consider mobility of user equipments (UEs) and URLLC requirement.

In addition to considering control overhead from handover delay, high-speed environment also induces carrier frequency offset (CFO) by Doppler shift phenomenon. The CFO destroys the orthogonality among subcarriers and generates additional interference for resource block (RB) in

the orthogonal frequency division duplexing (OFDM) systems and known as inter-carrier interference (ICI) in [17]. Recent algorithms design for mitigating interference from Doppler shift can be found in [18]. By exploiting position information, [18] proposes an ICI and multi-cell interference cancellation method using compressed channel estimation method, which is shown to be robust to the training speed. Nevertheless, [19] indicates that CFO in OFDM systems cannot be completely eliminated when employing latency reduction technique, such as physical-layer network coding for V2X communications with URLLC requirements. They suggest the necessity to consider interference incurred by Doppler shift when designing resource allocation algorithm for V2I networks.

Motivated by aforementioned literatures, this paper develops resource allocation algorithm for V2I networks with IBFD wireless backhaul. The formulated problem aims to maximize total throughput under reliability and latency constraints in backhaul links and access links respectively by jointly optimizing VUE association (VA), RB assignment (RA) and power allocation (PA). A matching-coalition game (MCG) method is proposed to handle complex objective function through pre-defined system preferences. The matching game (MG) provides a distributed self-organizing and self-optimizing approach for solving combinatorial problems of wireless resources in two disjoint sets, which is able to reduce both the coordination among SBSs and the capacity burden on backhaul links [20]. In comparison, coalition game (CG) is well-known for its property to perform interference management altruistically by cooperation among SBSs [21]. Hence, the proposed MCG scheme combines the MG and CG by offering a solution to strike a balance between overhead and capacity gain from coordination among SBSs. The main contributions of this paper are summarized as follows.

- A novel handover delay model is designed in this paper. The proposed model provides a tractable tool to consider the influence of handover delay when designing resource allocation algorithm for the network that involves UEs with high-speed mobility.
- To the best of the authors' knowledge, this paper is the first work to design resource allocation algorithm for networks under IBFD scheme with guaranteed URLLC service, while considering factors that result from the mobility of VUEs simultaneously, i.e., including RB interference caused by Doppler shift and handover delay.
- Since the converted objective function is non-convex and obtaining globally optimal solution is challenging, a low-complexity MCG algorithm based on MG and CG is proposed after separating discrete and continuous variables. The proposed MCG method is proved to achieve Nash-stable coalition structure and local optimality for RA and PA sub-problems respectively.
- The main novelty of this paper lies in the approach for RB assignment problem. To the best of the authors' knowledge, this paper is the first work to combine MCG method to solve the RB assignment problem in access links. In current literatures, RB assignment scheme is based on only MG theory [22] aiming to develop an
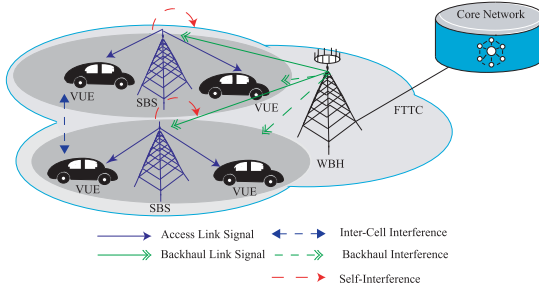
Fig. 1.   In-band full-duplex based vehicular to infrastructure networks.

algorithm with practical complexity, whereas MCG is applied to a simpler problem such as channel assignment problem in device-to-device (D2D) network [23]. In D2D network, each user is only allocated with one channel. Thus, a variant of join rule that decides whether a user should use a given channel is sufficient for the problem. In comparison, each VUE can use multiple RBs in this paper. It means that in addition to join rule, it is necessary to design rules that either consider the interference power caused to the entire network when a VUE uses a particular RB or allow different VUEs to exchange RBs. To tackle these considerations, this paper additionally introduces the departure, replacement and switch rules. These are redesigned and unique operations that enable the proposed algorithm to achieve superior performance compared to the baseline schemes in [22]. The principle of the proposed scheme can be applied to solve RB assignment problem in different networks, which provides an important basis for the upcoming resource allocation problem.

The rest of the paper is organized as follows. Section II describes the system model and the problem formulation. Section III introduces the proposed MCG-based algorithm. The theoretical analysis is discussed in Section IV. Section V provides numerical results to illustrate the performance of MCG method. Finally, the conclusions is made in Section VI. The key notations are summarized in Table I.

II. SYSTEM MODEL AND PROBLEM FORMULATION

As shown in Fig. 1, we consider an IBFD-based V2I OFDM networks consisting of N SBSs, a wireless backhaul hub (WBH), and K VUEs, which are equipped with N_S, N_B and single antenna, respectively. Additionally, SCN is considered instead of distributed massive MIMO to comprehensively investigate the factors from VUEs' mobility on system performance, including Doppler shift and handover delay. In addition, SCN is a widely adopted architecture in LTE-A networks and is expected to be utilized in 5G wireless network [24]. By contrast, the effect of handover cannot be reflected in distributed massive MIMO network since its corresponding VUEs are centrally managed. Centralized architecture may also not be applicable to fulfill URLLC service because managing large number of base stations causes huge signaling overhead and additional latency on backhaul links [15]. We assume that $N_S = N_T + N_R$, where N_T and N_R respectively represent the number of transmit and receive

TABLE I
SUMMARY OF THE MAIN NOTATIONS AND DEFINITIONS

Variable	Definition
N	Number of SBS
K	Number of VUE
J	Number of RB
$\Gamma_{n,j,k}(t)$	SINR of k-th VUE when associated with j-th RB of n-th SBS
$\Gamma_{b_j}(t)$	SINR of j-th RB in backhaul link
$R_k(t)$	Total throughput of k-th VUE
$\tilde{R}_k(t)$	Equivalent expression of $R_k(t)$
R_{req_k}	Throughput requirement for the k-th VUE
$x_{n,k}(t)$	VUE association variable for the k-th VUE and n-th SBS
$\alpha_{n,j,k}(t)$	RB association variable for the k-th VUE and j-th RB of n-th SBS
$p_{n,j}(t)$	Power allocation variable for the j-th RB of n-th SBS
$\eta_{n,k}(t)$	Reduced fraction of time interval caused by handover delay
q_V	Quota on the maximum served VUE for each SBS
$p_{\max}$	Maximum transmission power for each SBS
$\mathrm{BLER}_{b_j}(t)$	Block error rate of j-th RB in backhaul link
$B_{\max}$	Maximum tolerable block error rate
$d_k(t)$	Transmission delay of k-th VUE
d_{req}	Transmission delay requirement
$I_{\mathrm{SI}_j}(t)$	SI power of j-th RB in backhaul link
$I_{\mathrm{req}_{j,l}}$	Tolerable SI power of j-th RB
$U_{k,c}^V$	Utility function of k-th VUE when using radio resource c
$U_{c,k}^R$	Utility function of radio resource c when utilized by k-th VUE
Φ_j	The set of VUEs that utilizes RB j
Ω_k	The set of RBs that utilized by VUE k
Ψ_k	The index of associated SBS for VUE k
$U_r^C(\Phi_j)$	Utility function of the coalition Φ_j
$U_v^C(\Omega_k)$	Utility function of the coalition Ω_k

antennas. The considered network operates in a time-slotted manner with the slot duration normalized to integer unit, i.e., slot t refers to $[t, t+1)$, $t \in \{0, 1, 2, \cdots\}$. Without loss of generality, it is considered in this paper that wireless service requirements are sent by VUEs to some servers on the Internet at time slot $t = 0$, where the size of the required contents are denoted as $\mathcal{F} = \{F_1, F_2, \cdots, F_K\}$ and F_k represents the content size required by the k-th VUE. After receiving service request, transmissions of the required data $\mathcal{F}$ begins from $t = 1$ using one of the L kinds of modulation and coding schemes (MCSs), while VUEs move with chosen directions and speeds simultaneously. Specifically, the moving direction and speed of the k-th VUE in time slot t are denoted as $\phi_k(t)$ and $v_k(t)$, respectively.

Moreover, $\mathcal{F}$ are firstly transmitted to the WBH from the core network via fiber-to-the-cell (FTTC) links and SBSs are connected to core network through WBH. Hence, the delivery of $\mathcal{F}$ to corresponding VUEs is completed via three node transmission, including backhaul links from the WBH

to SBSs and access links from SBSs to VUEs, in which backhaul links and access links are established by the WBH and SBSs respectively using the same set of resource blocks (RBs) $\mathcal{J} = \{1, 2, \cdots, J\}$. Besides, RB allocation results of backhaul links $\boldsymbol{\beta}(t) = \{\beta_{1,1}(t), \cdots, \beta_{J,N}(t)\}$ are determined by the WBH. The parameter $\beta_{j,n}(t) \in \{0, 1\}$ is a binary indicator, where $\beta_{j,n}(t) = 1$ indicates that the j-th RB is allocated for the backhaul link between the n-th SBS and the WBH at time slot t. Note that an example of a WBH can be the macro base stations connected to the core network by FTTC links [13]. Furthermore, for the purpose of clarity, it is noteworthy that the intractability of resource management for the considered IBFD based network mentioned above is twofold: (i) The three node transmission and the fact that both backhaul links and access links utilize the same set of RBs give rise to backhaul interference (from WBH to VUEs) and SI (from access links to backhaul links on SBSs) besides the inter-cell interference in the conventional multi-cell networks; and (ii) Doppler shift resulting from VUEs' mobility destroys the orthogonality between RBs and induces additional RB interference to each RB.

In the presence of aforementioned interferences, the signal-to-interference-plus-noise ratio (SINR) of the k-th VUE associated with the j-th RB of the n-th SBS can be written as

$$\Gamma_{n,j,k}(t) = \frac{d_{n,j,k}(t)}{I_{\mathrm{t}_{n,j,k}}(t) + \sigma_{n,j,k}^2}, \tag{1}$$

where $d_{n,j,k}(t)$ is the power of desired signals from the n-th SBS on the j-th RB to the k-th VUE which is given as $d_{n,j,k}(t) = p_{n,j}(t)\|\mathbf{g}_{n,j,k}(t)\|^2$, where $p_{n,j}(t)$ is the transmission power of the j-th RB allocated by the n-th SBS. $\mathbf{g}_{n,j,k}(t) = \sqrt{s_{n,k}(t)}\boldsymbol{v}_{n,j,k}(t) \in \mathbb{C}^{N_T}$ is the channel vector between the j-th RB of the n-th SBS and the k-th VUE. $s_{n,k}(t) \in \mathbb{C}$ and $\boldsymbol{v}_{n,j,k}(t) \in \mathbb{C}^{N_T}$ are pathloss effect and fast fading, respectively. In (1), $I_{\mathrm{t}_{n,j,k}}(t)$ is the total interference power experienced by the k-th VUE when receiving data from the j-th RB of the n-th SBS and can be expressed as

$$I_{\mathrm{t}_{n,j,k}}(t) = I_{\mathrm{b}_{j,k}}(t) + I_{\mathrm{c}_{n,j,k}}(t) + \frac{I_{\mathrm{r}_{n,j}}(t)}{\delta_{\mathrm{r}}}, \tag{2}$$

where δ_{r} is the algorithm parameter used to characterize the capability of RB interference cancellation. $I_{\mathrm{b}_{j,k}}(t)$ is the backhaul interference from the j-th RB of WBH to the k-th VUE, which can be written as $I_{\mathrm{b}_{j,k}}(t) = p_{\mathrm{b}_j}(t)\|\mathbf{h}_{j,k}(t)\|^2$, where $p_{\mathrm{b}_j}(t)$ is the transmission power of the j-th RB allocated by the WBH, $\mathbf{h}_{j,k}(t) \in \mathbb{C}^{N_B}$ is the channel vector between the j-th RB of WBH and the k-th VUE. $I_{\mathrm{c}_{n,j,k}}(t)$ in (2) denotes the inter-cell interference to the k-th VUE from the other SBSs processing the signals from the j-th RB of the n-th SBS and is given by

$$I_{\mathrm{c}_{n,j,k}}(t) = \sum_{m=1, m \neq n}^{N} \sum_{u=1, u \neq k}^{K} \alpha_{m,j,u}(t) p_{m,j}(t)\|\mathbf{g}_{m,j,k}(t)\|^2, \tag{3}$$

where the parameter $\alpha_{m,j,u}(t) \in \{0, 1\}$ is a binary indicator and $\alpha_{m,j,u}(t) = 1$ indicates that the j-th RB of the m-th

SBS is allocated to the u-th VUE. $I_{\mathrm{r}_{n,j}}(t)$ in (2) is total RB interference power caused by Doppler shift to the j-th RB of the n-th SBS, which is expressed as

$$I_{\mathrm{r}_{n,j}}(t) = \sum_{k=1}^{K} \sum_{i=1, i \neq j}^{J} \alpha_{n,i,k}(t)\hat{I}_{\mathrm{r}_{n,i,j}}(t) + \check{I}_{\mathrm{r}_{n,j}}(t), \tag{4}$$

where $\hat{I}_{\mathrm{r}_{n,i,j}}(t)$ and $\check{I}_{\mathrm{r}_{n,j}}(t)$ represent the inter-RB interference from the i-th RB of the n-th SBS to the j-th RB of the n-th SBS and the intra-RB interference to the j-th RB of the n-th SBS, respectively, which can be expressed as [25]

$$\hat{I}_{\mathrm{r}_{n,j}}(t) = \Delta S \sum_{m=1}^{M} \sum_{h=1, h \neq m}^{M} \frac{1}{[(Mi + h) - (Mj + m)]^2}, \tag{5}$$

and

$$\check{I}_{\mathrm{r}_{n,j}}(t) = \Delta S \sum_{m=1}^{M} \sum_{h=1, h \neq m}^{M} \frac{1}{(h - m)^2}, \tag{6}$$

where $\Delta S = S \cdot \frac{\left(f_{d_k}(t)T_s\right)^2}{2}$ with S and M representing the number of OFDM symbols and the number of subcarriers in each RB, respectively. $f_{d_k}(t) = \frac{v_k(t)f_c}{v_c}$ is the maximum Doppler frequency. f_c and v_c are the carrier frequency and velocity of light respectively. T_s is the duration of an OFDM symbol. Note that (4) implies that there is no inter-RB interference from the i-th RB of the n-th SBS to the j-th RB of the n-th SBS, if the i-th RB of the n-th SBS is not assigned to serve any VUE. $\sigma_{n,j,k}^2$ in (1) is the AWGN experienced by VUE k when it is associated with the j-th RB of the n-th SBS.

When given the SINR of (1), the capacity of the k-th VUE on condition that it is associated with the n-th SBS over the j-th RB can be expressed as $\gamma_{n,j,k}(t) = w \log_2 \left(1 + \Gamma_{n,j,k}(t)\right)$, where w is the bandwidth of an RB. Total throughput of the k-th VUE in the considered network are given as

$$R_k(t) = \sum_{n=1}^{N} \sum_{j=1}^{J} x_{n,k}(t)\alpha_{n,j,k}(t)\eta_{n,k}(t)\gamma_{n,j,k}(t), \tag{7}$$

where $x_{n,k}(t) \in \{0, 1\}$ is a binary indicator with $x_{n,k}(t) = 1$ indicating that the k-th VUE is associated with the n-th SBS. $\eta_{n,k}(t)$ is the time interval for data transmission when the k-th VUE is connected with the n-th SBS and can be written as $\eta_{n,k}(t) = 1 - \iota_{n,k}(x_{n,k}(t-1) \oplus 1)$, where $\iota_{n,k} = \frac{\psi_{n,k}}{D_{n,k}} \in [0, 1]$ is the reduced fraction of time interval for data transmission caused by handover delay when the k-th VUE requires association with the n-th SBS from other SBSs, $D_{n,k}$ and $\psi_{n,k}$ are the duration of coherence time and handover delay between the n-th SBS and the k-th VUE respectively. The notation $\oplus$ is the exclusive or operator. For fixed n in (7), if $x_{n,k}(t-1) = 0$, then $\eta_{n,k}(t) = 1 - \iota_{n,k}$, which implies that handover will occur. In this case, a part of time interval for data transmission will be consumed by the control overhead from handover delay when the k-th VUE is not associated with the n-th SBS at the previous time slot $t-1$. In comparison, if $x_{n,k}(t-1) = 1$, then $\eta_{n,k}(t) = 1$, which indicates that the transmission rate will not be degraded by

handover delay when the k-th VUE has already connected with the n-th SBS at time slot $t-1$. Hence, whether VUE k is associated with SBS n in the previous time slot determines the occurrence of the handover at current time. The handover scheme in this paper can be regarded as hard handover based on constraint (12). $\eta_{n,k}(t)\gamma_{n,j,k}(t)$ in (7) is referred to as the effective transmission rate (ETR) in this paper and can be explained as the transmission rate from the j-th RB of the n-th SBS to VUE k when handover delay is taken into consideration. Note that (7) also implies that total throughput $R_k(t)$ of the k-th VUE is equal to the sum of ETR from all RBs of SBSs in the considered network. Thus, $R_k(t)$ in (7) can also be regarded as the total ETR of VUE k. Moreover, the reliability of backhaul link provided by the j-th RB with the l-th MCS is characterized by the block error rate (BLER) and is given as [1] $\text{BLER}_{\text{b}_j}(t) = \xi_l \exp(-\zeta_l \Gamma_{\text{b}_j}(t))$, where ζ_l and ξ_l are MCS-dependent constant. Note that the commonly-adopted reliability models in the existing literatures are developed based on: (1) conventional outage probability [8]; (2) extreme value theory to characterize the probability of maximal queue length exceeding a predefined threshold [6]; and (3) analytical result in [26] to characterize the relationship among the blocklength, coding rate and error probability [5]. It is worthwhile to mention that only the reliability model employed in this paper provides the insight between the adopted MCS and SI in the FD systems, which will be discussed in details in Section V-C. $\Gamma_{\text{b}_j}(t)$ is SINR of j-th RB in backhaul link and is given as

$$\Gamma_{\text{b}_j}(t) = \frac{d_{\text{b}_j}(t)}{I_{\text{SI}_j}(t) + \sigma_{\text{b}_j}^2}. \tag{8}$$

$\sigma_{\text{b}_j}^2$ is the AWGN in the backhaul link provided by the j-th RB, and the power of the desired signals from the j-th RB in backhaul links is $d_{\text{b}_j}(t) = \sum_{n=1}^{N} \beta_{j,n}(t) p_{\text{b}_j(t)} \|\mathbf{h}_{\text{b}_{j,n}}(t)\|^2$, where $\mathbf{h}_{\text{b}_{j,n}}(t) \in \mathbb{C}^{N_R \times N_B}$ is channel matrix between j-th RB of the WBH and n-th SBS. In (8), $I_{\text{SI}_j}(t)$ is the SI power experienced by the j-th RB in backhaul links and can be expressed as

$$I_{\text{SI}_j}(t) = \sum_{n=1}^{N} \sum_{k=1}^{K} \alpha_{n,j,k}(t) p_{n,j}(t) \|\mathbf{G}_{\text{SI}_{n,j}}(t)\|^2 / \delta_{\text{SI}}, \tag{9}$$

where $\mathbf{G}_{\text{SI}_{n,j}}(t) \in \mathbb{C}^{N_R \times N_T}$ is the SI channel matrix from the access links of n-th SBS to j-th RB in backhaul links. Note that since this paper is the first work that considers V2I networks under the IBFD backhauling scheme, global knowledge of CSI is assumed to provide performance upper bound for the considered networks. In practical networks, the inter-cell interference and backhaul interference can be treated as the part of thermal noise as indicated in [27]. Other types of CSI, e.g., DL and UL, can be obtained by adopting exchanging mechanism between SBS and VUE in [28], which is considered as a feasible procedure. In addition, recent channel estimation technique in [29] indicates that CSI collection is viable even when the velocity is up to 80 km/h. Hence, channel estimation can be robust enough in vehicular networks. δ_{SI} in (9) is the algorithm parameter used to represent the ability of SI cancellation algorithm. Note that the solution to overcome

SI can be found in our previous work [16] and other existing literatures [30]. Although SI cancellation methods have been widely investigated, the SI cannot be completely eliminated by the current signal processing technique. Hence, by reusing the scheme of our previous work in [16], the motivation to incorporate FD systems in this paper is to enhance FD system performance through resource allocation method with considered FD systems including the practical implementations, i.e., SI cancellation capability. As shown in Fig. 2 in Section V, the proposed MCG method provides noticeable performance gain compared with the scheme without proper resource allocation. The throughput gain in Fig. 2 indicates that appropriate resource allocation is a viable solution to enhance FD system performance. In addition, each SBS serves VUEs by assigning RBs with pre-defined quota on the maximum number of served VUEs and the total transmission power, whereas each VUE can only be associated with one SBS. Besides, each RB of a given SBS can only be assigned to one VUE. The corresponding constraints are given as

$$\sum_{k=1}^{K} x_{n,k}(t) \le q_{\text{V}}, \forall n, \tag{10}$$

$$\sum_{j=1}^{J} p_{n,j}(t) \le p_{\max}, \forall n, \tag{11}$$

$$\sum_{n=1}^{N} x_{n,k}(t) \le 1, \forall k, \tag{12}$$

and

$$\sum_{k=1}^{K} \alpha_{n,j,k}(t) \le 1, \forall n, j, \tag{13}$$

where q_{V} and $p_{\max}$ are respectively quota on the maximum number of served VUEs and total transmission power for each SBS.

With all the above preparation, the considered optimization problem aiming to maximize VUEs' total throughput can be described as

$$\max_{\mathbf{x}, \boldsymbol{\alpha}, \mathbf{p}} \sum_{k=1}^{K} R_k(t) \tag{14a}$$

$$\text{subject to} \quad (10) - (13)$$

$$\text{BLER}_{\text{b}_j}(t) \le B_{\max}, \forall j, \tag{14b}$$

$$d_k(t) \le d_{\text{req}}, \forall k, \tag{14c}$$

$$\alpha_{n,j,k}(t) \in \{0,1\}, \forall n, j, k, \tag{14d}$$

$$x_{n,k}(t) \in \{0,1\}, \forall n, k, \tag{14e}$$

where $\mathbf{x} = \{x_{n,k}\}, \boldsymbol{\alpha} = \{\alpha_{n,j,k}\}, \mathbf{p} = \{p_{n,k}\}, \forall n, j, k$ are symbolic notations of the design variables specifically for VA, RA and PA respectively. $B_{\max}$ is the maximum tolerable BLER. d_{req} is the required latency. $d_k(t) = \frac{F_k}{R_k(t)}$ is the transmission delay of the k-th VUE. (14d) and (14e) are the constraints for the binary indicators $\alpha_{n,j,k}(t)$ and $x_{n,k}(t)$, respectively.

III. RESOURCE ALLOCATION ALGORITHM DESIGN

The formulated problem in (14) is a mixed integer non-linear problem with non-convex objective function and constraints. Hence, searching for its globally optimal solution is

difficult and induces huge computational burden in general. To the best of the authors' knowledge, finding globally optimal solution for non-convex problem similar to (14) is still an open problem [31]. In order to develop tractable solution, this section firstly applies a relaxation method to reformulate the considered problem (14) based on equivalent expression of the objective function (14a). The equivalent expression converts the original objective function into the form involving only RA and PA variables. A MCG-based algorithm is then proposed to solve the reformulated problem. The merit of the proposed MCG-based method comes from its ability to exploit particular structure of the reformulated problem and gives rise to simple sub-problems in each iteration. With the aid of the MCG-based algorithm, constraints involving binary optimization variables can be handled by decomposing the reformulated problem into two sub-problems: (a) *RA sub-problem*, which is a mixed integer programming (MILP) involving discrete variable $\boldsymbol{\alpha}$; and (b) *PA sub-problem*, which is a non-convex problem involving continuous optimization variable $\mathbf{p}$. Specifically, the RA sub-problem is solved for a given set of $\mathbf{p}$, while solution for PA sub-problem is searched under determined $\boldsymbol{\alpha}$. For the RA sub-problem, the MG theory is firstly applied to associate each VUE with multiple SBSs. After the matching results yield at least one SBS that can satisfy the data rate constraint, the SBS that provides the highest ETR for a given VUE is then selected to be the serving SBS by VA decision scheme. The CG method is finally utilized to tackle the influence of inter-cell interference and determine RA policy. After the RA sub-problem is solved, the DC method is used to search for the solutions of the PA sub-problem. The RA and PA sub-problems are solved iteratively until the converging condition is satisfied.

A. Problem Reformulation

The following proposition is obtained for reformulating of the considered problem.

Proposition 1: The throughput $R_k(t)$ in objective function (14a) can be equivalently written as

$$\tilde{R}_k(t) = \sum_{n=1}^{N} \sum_{j=1}^{J} \alpha_{n,j,k}(t)\eta_{n,k}(t)\gamma_{n,j,k}(t). \tag{15}$$

Proof: Given a fixed set of SBS, RB and VUE indices n, j and k, Proposition 1 can be proved by showing that the allocation of ETR $\eta_{n,k}(t)\gamma_{n,j,k}(t)$ depends only on the variable $\alpha_{n,j,k}(t)$. Based on the nature of its physical meaning, $x_{n,k}(t) = 1$ whenever $\alpha_{n,j,k}(t) = 1$. Thus, $\eta_{n,k}(t)\gamma_{n,j,k}(t)$ will be allocated to VUE k when $\alpha_{n,j,k}(t) = 1$. By contrast, $\eta_{n,k}(t)\gamma_{n,j,k}(t)$ will not be allocated to VUE k when $\alpha_{n,j,k}(t) = 0$ and $x_{n,k}(t) = 1$ from $R_k(t)$ in (7). Hence, it can be seen that the allocation of ETR $\eta_{n,k}(t)\gamma_{n,j,k}(t)$ is determined only by the variable $\alpha_{n,j,k}(t)$, which completes the proof. ∎

Note that constraints (10) and (12) cannot be precisely described if only a single RB assignment variable is taken into account. For instance, when $q_V = 5$, if the association variable is replaced by only adopting the RB assignment variable, the constraint (10) is given as $\sum_{j=1}^{J} \sum_{k=1}^{K} \alpha_{n,j,k}(t) \leq q_V, \forall n$,

which means that each SBS can use at most 5 RBs for access link transmissions to limit the number of associated VUE to be less than 5, which results in different physical meaning with the original problem in this paper. Thus, the association variable is non-negligible.

By applying Proposition 1 and removing the constraints (10) and (12) that are related to VA, the optimization problem can be reformulated as

$$\max_{\boldsymbol{\alpha},\mathbf{p}} \sum_{k=1}^{K} \tilde{R}_k(t) \tag{16a}$$

subject to (11), (13) and (14d)

$$I_{\mathrm{SI}_j}(t) \leq I_{\mathrm{req}_{j,l}}, \forall j, l, \tag{16b}$$

$$\tilde{R}_k(t) \geq R_{\mathrm{req}_k}, \forall k, \tag{16c}$$

where $I_{\mathrm{req}_{j,l}} = d_{b_j}(t) \cdot \left(-\frac{\zeta_l}{\ln(B_{\max}/\xi_l)} \right) - \sigma_{b_j}^2$. $I_{\mathrm{req}_{j,l}}$ can be interpreted as the tolerable SI power of backhaul link provided by j-th RB under l-th MCS scheme. $R_{\mathrm{req}_k} = F_k/d_{\mathrm{req}}$. Constraints (16b) is obtained by combining $\mathrm{BLER}_{b_j}(t)$ and (14b), whereas (16c) is attained from (14c) and Proposition 1. The considered problem (16) involves system throughput maximization and a QoS constraint due to the equation (16a) and (16c).

Remark 1: It should be noted that the optimization problem (16) implies that the original reliability and latency constraints can be described as SI threshold and throughput requirements as shown in (16b) and (16c) respectively in the considered network. Moreover, since the optimization problem (16) involves only RB assignment $\boldsymbol{\alpha}$ and power allocation $\mathbf{p}$, it can be seen that computational complexity is reduced after the reformulation of the problem. Besides, by setting the transmission rate of backhaul links based on (8) as an objective function and backhaul interference threshold based on $I_{b_{j,k}}(t)$ as a constraint, a dynamic PA at the WBH can be directly obtained based on the proposed PA scheme in this paper. Note that such problem is a simplified version of our original problem since it only has one constraint and (8) only contains one interference term, i.e., the SI. This problem is not presented in this paper due to page limitation. Constraint (16c) implies that the influence of backhaul interference and other interferences to each VUE is mitigated by providing sufficient data rate.

B. Algorithm Design for RA Sub-Problem

After the original optimization problem is reformulated, the RA sub-problem is given as follows.

$$\max_{\boldsymbol{\alpha}} \sum_{k=1}^{K} \tilde{R}_k(t)$$

subject to (13), (14d), (16b) and (16c). $\tag{17}$

Note that each VUE can use multiple RBs, and each RB of a given SBS can only be assigned to one VUE. Therefore, the RA sub-problem can be modeled as a many-to-one MG and solved by MG theory, which tackles combinatorial optimization problem by matching players in two sets based on its

list of preference utility. To develop an MG for the RA sub-problem, the definition of matching is provided as follows.

Definition 1 (Matching): Let $\mathcal{K} = \{1, 2, \cdots, K\}$ and $\mathcal{C} = \{1, 2, \cdots, NJ\}$ represent the sets of VUEs and radio resources (RRs) of all SBSs, respectively. A matching is defined as the result of bidirectional mapping between the sets $\mathcal{K}$ and $\mathcal{C}$ via functions μ_{u} and μ_{r} such that

(a.) $\forall k \in \mathcal{K}$, we have $\mu_{\mathrm{u}}(k) \in \mathcal{C}$ and $|\mu_{\mathrm{u}}(k)| \in \{0, \cdots, NJ\}$.
(b.) $\forall c \in \mathcal{C}$, we have $\mu_{\mathrm{r}}(c) \in \mathcal{V}$ and $|\mu_{\mathrm{r}}(c)| \in \{0, 1\}$.

$|\mu_{\mathrm{u}}(\cdot)|$ represents the cardinality of matching outcome $\mu_{\mathrm{u}}(.)$. Notice that each RR $c \in \mathcal{C}$ has a corresponding pair (n, j) that represents its indices of SBS and RB. For instance, $(n, j) = (N, J)$ when $c = NJ$, which means that it denotes the J-th RB of N-th SBS. Moreover, when a VUE $k \in \mathcal{K}$ does not use any RRs or an RR $c \in \mathcal{C}$ is not assigned to any VUEs, we have $\mu(k) = \emptyset$ or $\mu(c) = \emptyset$.

For any VUEs $k \in \mathcal{K}$, it aims to choose RR c with corresponding pair (n, j) that can maximize its ETR. Hence, the utility function of VUE k on RR c can be represented as $U_{k,c}^{\mathrm{V}} = \eta_{n,k}\gamma_{n,j,k}$. It should be noted that $\eta_{n,k}(t)$ and $\gamma_{n,j,k}(t)$ in (15) are written as $\eta_{n,k}$ and $\gamma_{n,j,k}$ in $U_{k,c}^{\mathrm{V}}$ and the notation for the index of time slot "(t)" will be omitted in the rest of this paper for brevity. Meanwhile, RR c with corresponding pair (n, j) intends to serve VUEs k with highest received signal power to maximize the sum rate of its corresponding SBS [22]. Thus, the preference utility of RR c to accept VUE k can be described as $U_{c,k}^{\mathrm{R}} = p_{n,j}\|\mathbf{g}_{n,j,k}\|^2$. To rank preference utility of VUEs or RRs, a preference relation is introduced as follows.

Definition 2 (Preference Relation $\succ$): A preference relation $\succ$ is a binary relation that is used to compare and specify the utilities between players in $\mathcal{K}$ and $\mathcal{C}$, which satisfies complete, reflexive and transitive properties [32]. A strict preference relation $\succ_c$ is defined over the set of RRs such that when given a VUE k, two RRs c_1 and $c_2 \in \mathcal{C}$, $c_1 \neq c_2$, we have $c_1 \succ_k c_2 \Leftrightarrow U_{k,c_1}^{\mathrm{V}} > U_{k,c_2}^{\mathrm{V}}$. Similarly, a strict preference relation $\succ_c$ is defined over the set of VUEs $\mathcal{K}$ such that given a RR c, two VUEs k_1 and $k_2 \in \mathcal{K}$, $k_1 \neq k_2$, we have $k_1 \succ_c k_2 \Leftrightarrow U_{c,k_1}^{\mathrm{R}} > U_{c,k_2}^{\mathrm{R}}$. With the definition of preference utility functions $U_{k,c}^{\mathrm{V}}$, $U_{c,k}^{\mathrm{R}}$ and of preference relations $\succ_k$, $\succ_c$, players, i.e., VUEs and RRs, can build their own preference list and solve the RA sub-problem by MG, which is defined as follows.

Definition 3 (Matching Game): An MG is defined by the tuple $(\mathcal{K}, \mathcal{C}, \succ_k, \succ_c)$ containing two sets of players and two preference relations, which allows each player to build its own preference list and find its final matching.

The proposed iterative MG algorithm is summarized in Algorithm 1. Initially, each VUE is assigned with κ_{ini} RRs based on its received signal power. The preference list for VUE k over RRs, i.e., Ψ_k^{MG}, is built according to utility function $U_{k,c}^{\mathrm{V}}$ and sorted by preference relation $\succ_k$ (line 1). VUE k then contacts and checks whether it can get matched with its most preferred RR c. If RR c has been used by another VUE k' based on Φ_c^{MG}, which is the index of the VUE using the RR c, the preference utilities of RR c over VUEs k and k' are calculated based on utility function $U_{c,k}^{\mathrm{R}}$ and compared by

preference relation $\succ_c$. The VUE with lower preference utility will be discarded/rejected and propose to the next preferred RR after removing RR c from its preference list to avoid proposing to the same RR again (lines 2 to 14). By contrast, VUE k can get matched with RR c if constraint (16b) is not violated after the matching is permitted when RR c is not occupied by any VUEs (lines 15 to 18). The matching process is repeated iteratively until the termination condition $\bar{R}_k - R_{\mathrm{req}_k} > \epsilon_{\mathrm{mat}}$ is satisfied (line 23), where ϵ_{mat} represents convergence threshold. $\bar{R}_k(t) = \max\{R_{n,k}(t)\}, 1 \leq n \leq N$. $R_{n,k}(t) = \sum_{j=1}^{J} \alpha_{n,j,k}(t)\eta_{n,k}(t)\gamma_{n,j,k}(t)$ represents the data rate provided by the n-th SBS to the k-th VUE. Note that for a VUE k to keep RBs that can satisfy constraint (16b) in its preference list, each SBS has to transmit additional control signal to inform VUE k about whether its RBs are used in access link. This process will cause huge signaling overhead and is difficult to be implemented in the practical networks. Thus, whether constraint (16b) is satisfied is checked by SBS after a VUE proposes to an RB. Moreover, from (9), it can be seen that the SI power from the n-th SBS to backhaul link provided by the j-th RB is produced when the j-th RB of the n-th SBS is used for access link transmission, i.e., when $\sum_{k=1}^{K} \alpha_{n,j,k}(t) = 1$. The generated SI power go through the same SI channel matrix $\mathbf{G}_{\mathrm{SI}_{n,j}}(t)$ regardless of which VUE is served, because all SBSs implement omni-directional transmission. Hence, the satisfaction of constraint (16b) needs to be examined only under the circumstance that the contacted RR c is not used by any VUEs (line 14). After the implementation of Algorithm 1, an intermediate RA result can be acquired and denoted as α_{mat} based on both the matching result and the corresponding pair of each RR. The outcome for VA can be accordingly determined by α_{mat}. Let k^* denote the VA result of VUE k, which is given as

$$k^* = \arg \max_n \sum_{j=1}^{J} \alpha_{n,j,k}\eta_{n,k}\gamma_{n,j,k}. \tag{18}$$

In other words, we have

$$x_{n,k} = \begin{cases} 1, & \text{if } n = k^*, \\ 0, & \text{otherwise.} \end{cases} \tag{19}$$

Remark 2: The principle behind the proposed VA policy for VUEs is to associate SBS that will contribute highest total ETR $\sum_{j=1}^{J} \alpha_{n,j,k}\eta_{n,k}\gamma_{n,j,k}$ to the connected VUE, which agrees with intuitional understanding.

The process of VA decision is illustrated in Algorithm 2. After obtaining α_{mat}, k^* is chosen by (18) (line 5). If SBS k^* has served q_{V} VUEs, ETR for VUE k (χ_k^{VA}) and all its served VUE $k' \in \Omega_n^{\mathrm{VA}}$ is calculated, where Ω_n^{VA} is the served VUE for SBS k^*. Based on the calculated ETR, the SBS k^* discards/rejects association from the VUE with the lowest total ETR. The discarded/rejected VUE then eliminates all RBs of SBS k^* in α_{mat} such that it can update its VA result from (18) and implement Algorithms 1 and 2 again to search for another SBS. After associated SBS for VUE k is decided, the elements in $\boldsymbol{\alpha}_{\mathrm{mat}}$ has to be updated as $\alpha_{n',j,k} = 0, \forall n' \neq k^*$ to ensure that VUE k does not use RBs of other SBSs (lines 6 to 11). The VA decision algorithm is performed in an iterative manner

---

Algorithm 1 Iterative MG Algorithm

1: Initialization:
    1) Set parameters κ_{ini}, and ϵ_{mat}
    2) Each VUE is allocated with κ_{ini} RRs based on its received signal power
    3) Preference list Ψ_k^{MG} of VUE k over RRs is built
2: **repeat**
3:   **for** $k = 1$ to K **do**
4:     **if** $\bar{R}_k - R_{\mathrm{req}_k} \leq \epsilon_{\mathrm{mat}}$ **then**
5:       VUE k choose RR c such that $U_{k,c}^{\mathrm{V}} > U_{k,c'}^{\mathrm{V}}$ for all $c' \in \Psi_k^{\mathrm{MG}}$
6:       **if** $\Phi_c^{\mathrm{MG}} == k'$ **then**
7:         **if** $U_{c,k}^{\mathrm{R}} > U_{c,k'}^{R}$ **then**
8:           - $\Phi_c^{\mathrm{MG}} = k$
9:           - $\Psi_{k'}^{\mathrm{MG}} = \Psi_{k'}^{\mathrm{MG}} \setminus c$
10:         **else**
11:           - $\Phi_c^{\mathrm{MG}} = k'$
12:           - $\Psi_k^{\mathrm{MG}} = \Psi_k^{\mathrm{MG}} \setminus c$
13:         **end if**
14:       **else if** $\Phi_c^{\mathrm{MG}} \notin \mathcal{K}$ and constraint (16b) holds when $\Phi_c^{\mathrm{MG}} = k$ **then**
15:         - $\Phi_c^{\mathrm{MG}} = \Phi_c^{\mathrm{MG}}$
16:         - $\Psi_k^{\mathrm{MG}} = \Psi^{\mathrm{MG}} \setminus c$
17:       **else**
18:         - $\Phi_c^{\mathrm{MG}} = k$
19:       **end if**
20:     **end if**
21:   **end for**
22:   - Each VUE rebuilds its preference list based on current matching
23: **until** $\bar{R}_k - R_{\mathrm{req}_k} > \epsilon_{\mathrm{mat}}, \forall k$

Algorithm 2 VA Decision Algorithm

1: Initialization:
    1) Given RA result $\boldsymbol{\alpha}_{\mathrm{mat}}$ from Algorithm 1
2: **repeat**
3:   **for** $k = 1$ to K **do**
4:     **if** k^* is not decided **then**
5:       - Update k^* based on (18) from $\boldsymbol{\alpha}_{\mathrm{mat}}$
6:       **if** SBS k^* has served q_{V} VUEs **then**
7:         - SBS k^* calculates χ_k^{VA} and $\chi_{k'}^{\mathrm{VA}}$ for all $k' \in \Omega_n^{\mathrm{VA}}$
8:         - $\Omega_n^{\mathrm{VA}} = \Omega_n^{\mathrm{VA}} \setminus k'$ with $\chi_{k'}^{\mathrm{VA}} < \chi_{\tilde{k}}^{VA}$ for all $\tilde{k} \in \Omega_n^{\mathrm{VA}}$
9:       **else**
10:         - Update $x_{n,k}$ and RA result $\boldsymbol{\alpha}_{\mathrm{mat}}$ for VUE k based on (19)
11:       **end if**
12:     **end if**
13:   **end for**
14: **until** $\sum_{n=1}^{N} x_{n,k} = 1, \forall k$

---

considered network. Specifically, Φ_j and Ω_k represent the sets of VUEs and RBs that utilize RB j and are occupied by VUE k, respectively; while Ψ_k denotes the index of the associated SBS for VUE k.

The CG allows an SBS n to decide whether its serving VUE k can join or depart from a coalition based on corresponding rules by cooperating with other SBSs altruistically [21]. To better understand the process of the proposed CG method, the definitions of join rule, departure rule, replacement rule and switch rule are detailed as follow.

Definition 5 (Join Rule): Given VUE k, RB j and partitions $\{\boldsymbol{\Phi}, \boldsymbol{\Omega}, \boldsymbol{\Psi}\}$, such that $k \notin \Phi_j$ and $j \notin \Omega_p$, for all p with $\Psi_p = \Psi_k$, which implies that VUE k does not use RB j, and RB j is not used by any VUEs with the same associated SBS as VUE k. The VUE k has an incentive to join the coalition Φ_j if $U_{\mathrm{r}}^{\mathrm{C}}(\Phi_j') > U_{\mathrm{r}}^{\mathrm{C}}(\Phi_j)$, where

$$U_{\mathrm{r}}^{\mathrm{C}}(\Phi_j) = \begin{cases} \sum_{m \in \Phi_j} \sum_{n = \Psi_m} \chi_{n,j,m}, & \text{if (16b) is satisfied,} \\ 0, & \text{otherwise.} \end{cases} \quad (20)$$

$\chi_{n,j,m} = x_{n,m} \alpha_{n,j,m} \eta_{n,m} \gamma_{n,j,m}$ and $\Phi_j' = \Phi_j \cup k$. $U_{\mathrm{r}}^{\mathrm{C}}(\Phi_j)$ is the utility function of coalition Φ_j in the CG, which can be interpreted as the sum of the ETR when RB j is utilized by members in the coalition Φ_j.

Definition 6 (Departure Rule): Given VUE k, RB j and partitions $\{\boldsymbol{\Phi}, \boldsymbol{\Omega}, \boldsymbol{\Psi}\}$, such that $k \in \Phi_j$ and $j \in \Omega_k$, which indicate that VUE k is using RB j. The VUE k has an incentive to depart from the coalition Φ_j if the following conditions are satisfied: (1) $U_{\mathrm{r}}^{\mathrm{C}}(\Phi_j') > U_{\mathrm{r}}^{\mathrm{C}}(\Phi_j)$; (2) $U_{\mathrm{v}}^{\mathrm{C}}(\Omega_k') > \tilde{R}_{\mathrm{req}_k}$, where $\Phi_j' = \Phi_j \setminus k$, $\Omega_k' = \Omega_k \setminus j$ and $U_{\mathrm{v}}^{\mathrm{C}}(\Omega_k) = \sum_{n=\Psi_k} \sum_{j \in \Omega_k} \chi_{n,j,k}$. $U_{\mathrm{v}}^{\mathrm{C}}(\Omega_k)$ is the utility function of VUE k in the CG, which can be explained as total ETR of VUE k when it occupies RBs Ω_k.

Definition 7 (Replacement and Switch Rules): Given VUEs k and k', RB j as well as partitions $\{\boldsymbol{\Phi}, \boldsymbol{\Omega}, \boldsymbol{\Psi}\}$, such that

until the equality $\sum_{n=1}^{N} x_{n,k} = 1, \forall k$ holds (line 14), which means that all VUEs are associated with one SBS. Notice that constraints (10) and (12) has been taken into account in lines 6 and 14, respectively.

The outcome of Algorithms 1 and 2 produces mutually beneficial matching assignment among players. However, for any players $k \in \mathcal{K}$ in the MG, their matching results are dependent on the RA results of other players, which are known as externality. In the presence of externality, one player might find it beneficial for its throughput improvement to change its RA result when an MG is completed [32]. To be more specific, if an RB j is used by a small number of VUEs and only suffers from little inter-cell interference power, it would be beneficial for some VUEs in different SBSs to use the RB j to improve throughput of the entire network. In this regard, it is necessary to develop a mechanism to provide VUEs an opportunity to deviate from previously agreed matching decision and further improve the overall performance of the considered network. The behaviors of VUEs' deviation from current RA results can be modeled as a CG, which is defined as follows.

Definition 4 (Coalition Game): A coalition game is identified by the tuple $(\boldsymbol{\Phi}, \boldsymbol{\Omega}, \boldsymbol{\Psi})$, where $\boldsymbol{\Phi} = \{\Phi_1, \Phi_2, \cdots \Phi_J\}$, $\boldsymbol{\Omega} = \{\Omega_1, \Omega_2, \cdots \Omega_K\}$, and $\boldsymbol{\Psi} = \{\Psi_1, \Psi_2, \cdots \Psi_K\}$ are the partitions of VUEs, RBs and SBSs, respectively, in the

---

Algorithm 3 Iterative CG Algorithm

1: Initialization:
   1) Set parameters $\boldsymbol{\Phi}$, $\boldsymbol{\Psi}$ and $\boldsymbol{\Omega}$, iteration index h_{coa} and convergence threshold τ_{coa}
2: **repeat**
3:   Randomly choose VUE k RB j
4:   **if** $k' \notin \Phi_j \; \forall \; k'$ with $\Psi_{k'} = \Psi_k$ **then**
5:     - VUE k applies $\mathcal{R}_J$ for Φ_j
6:   **else if** $k \in \Phi_j$ **then**
7:     - VUE k applies $\mathcal{R}_D$ for Φ_j
8:   **else if** $\exists \; k' \in \Phi_j$ with $\Psi_{k'} = \Psi_k$ and **then**
9:     - VUE k applies $\mathcal{R}_R$ or $\mathcal{R}_S$ for Φ_j
10: **end if**
11: **if** $\Omega'_k == \Omega_k$
     then
12:    - $h_{\text{coa}} = h_{\text{coa}} + 1$
13: **else**
14:    - $h_{\text{coa}} = 0$
15:    - Update $\boldsymbol{\Phi}$ and $\boldsymbol{\Omega}$
16: **end if**
17: **until** $h_{\text{coa}} \geq K \cdot \tau_{\text{coa}}$

$k' \in \Phi_j$, $j \in \Omega_{k'}$, $k \notin \Phi_j$, $j \notin \Omega_k$ and $\Psi_{k'} = \Psi_k$, which signifies that RB j is used by the VUE k' that associates with the same SBS as VUE k. The VUE k can use RB j by executing replacement operation (RO) on VUE k' or searching for another RB j', such that $j' \in \Omega_k$ and performing switch operation (SO) with VUE k' if the following conditions are satisfied: (1) $U_r^C(\Phi'_j) > U_r^C(\Phi_j)$; (2) $U_v^C(\Omega'_k)$, $U_v^C(\Omega'_{k'}) > \tilde{R}_{\text{req}_k}$; (3) $U_r^C(\Phi'_j) + U_r^C(\Phi'_{j'}) > U_r^C(\Phi_j) + U_r^C(\Phi_{j'})$, where

$$\Omega'_k = \begin{cases} \Omega_k \cup j, & \text{for RO,} \\ \Omega_k \cup j \setminus j', & \text{for SO,} \end{cases} \tag{21}$$

$$\Omega'_{k'} = \begin{cases} \Omega_{k'} \setminus j, & \text{for RO,} \\ \Omega_{k'} \setminus j \cup j', & \text{for SO,} \end{cases} \tag{22}$$

$$\Phi'_{j'} = \begin{cases} \Phi_{j'}, & \text{for RO,} \\ \Phi_{j'} \cup k' \setminus k, & \text{for SO,} \end{cases} \tag{23}$$

$$\text{and } \Phi'_j = \Phi_j \cup k \setminus k'. \tag{24}$$

Remark 3: The major difference between RO and SO can be observed from (21) and (22) that the cardinality of Ω'_k and $\Omega'_{k'}$ are increased and decreased respectively after RO is implemented, whereas the total number of elements in Ω'_k and $\Omega'_{k'}$ remain unchanged after SO. Additionally, since RO does not change elements in Ω_k, members in the coalition $\Phi_{j'}$ are updated only when SO is performed from (23). Besides, as the coalition Φ_j will go through the same members updating process in both RO and SO, coalition variation from Φ_j to Φ'_j does not need to be classified into different cases (i.e., either RO or SO) as shown in (24).

The procedure of proposed iterative CG algorithm is summarized in Algorithm 3. In each iteration, VUE k and the potentially joinable coalition Φ_j are randomly generated after parameter initialization (lines 1 to 3). If RB j is not used by any VUEs in the SBS Ψ_k, VUE k will try to join the coalition Φ_j by join rule ($\mathcal{R}_J$). Otherwise, departure rule ($\mathcal{R}_D$) or replacement/switch rule ($\mathcal{R}_R/\mathcal{R}_S$) will be applied when RB

j is used by VUE k or VUE k' in SBS Ψ_k, respectively. (lines 4 to 10). The iterative CG algorithm is terminated when the number of unsuccessful operations h_{coa} is equal to the product of the number of VUE in the considered network K and the convergence threshold τ_{coa} (lines 11 to 17), which is demonstrated to be a suitable criterion for CG to achieve stable partitions [28], [33].

Note that in some extreme cases, e.g., when $N \cdot q_V < K$, some VUEs might not be served. N is the number of SBS, q_V is the number of VUE that each SBS can serve, and K is total number of VUE in the network. In this situation, the proposed scheme can be combined with basic time slot allocation method to ensure that each VUE is served for equal time duration. Therefore, at least VUEs can have URLLC service when they are associated with an SBS, which is a reasonable solution to tackle dense traffic in the hotspot scenario.

C. Algorithm Design for PA Sub-Problem

By utilizing the solution of the RA sub-problem as stated in the previous subsection, the PA sub-problem can be simplified as

$$\max_{\mathbf{p}} \sum_{k=1}^{K} R_k(t)$$
$$\text{subject to (11), (16b) and (16c).} \tag{25}$$

To tackle the non-convexity of the objective function (7) and constraint (16c), the difference of convex (DC) function approach will be applied to convert the problem. The DC method is well-known for its robustness and efficient properties to handle non-convex problem compared to the other methods [34]. By adopting DC scheme and let $\rho_{n,j} = \log p_{n,j}$, the total ETR of VUE k in (7) can be rewritten as $R_k = f_k(\boldsymbol{\rho}) - h_k(\boldsymbol{\rho})$, where

$$f_k(\boldsymbol{\rho}) = \sum_{n=1}^{N} \sum_{j=1}^{J} \lambda_{n,j,k} \log_2(d'_{n,j,k} + I'_{t_{n,j,k}} + \sigma^2_{n,j,k}), \tag{26}$$

and

$$h_k(\boldsymbol{\rho}) = \sum_{n=1}^{N} \sum_{j=1}^{J} \lambda_{n,j,k} \log_2(I'_{t_{n,j,k}} + \sigma^2_{n,j,k}). \tag{27}$$

$\lambda_{n,j,k} = x_{n,k} \alpha_{n,j,k} \eta_{n,k}$. $I'_{n,j,k} = I'_{t_{n,j,k}} + \sigma^2_{n,j,k}$. $d'_{n,j,k}$ and $I'_{t_{n,j,k}} = I_{b_{j,k}} + I'_{c_{n,j,k}} + \frac{I_{r_{n,j}}}{\delta_r}$ are the power of desired signals from n-th SBS on j-th RB to k-th VUE and total interference power experienced by k-th VUE when receiving data from j-th RB of n-th SBS as shown in $d_{n,j,k}(t)$ and (2), respectively. After applying variable transformation $\rho_{n,j} = \log p_{n,j}$, the following two terms can be expressed as $d'_{n,j,k} = e^{\rho_{n,k}} \|\mathbf{g}_{n,j,k}\|^2$, and

$$I'_{c_{n,j,k}} = \sum_{m=1, m \neq n}^{N} \sum_{u=1, u \neq k}^{K} \alpha_{m,j,u} e^{\rho_{m,j}} \|\mathbf{g}_{m,j,k}\|^2. \tag{28}$$

Hence, the PA sub-problem can be reformulated as

$$\max_{\boldsymbol{\rho}} \sum_{k=1}^{K} f_k(\boldsymbol{\rho}) - h_k(\boldsymbol{\rho}) \tag{29a}$$

Algorithm 4 Iterative DC Algorithm

1: Initialization:
    1) Set iteration index h_{dc}, the convergence threshold ϵ_{dc} and initialize $\boldsymbol{\rho}^0$
2: **repeat**
3:     Solve (30) and denote the optimal solution as $\boldsymbol{\rho}^*$
4:     Update $\boldsymbol{\rho}^* = \boldsymbol{\rho}^{h_{\mathrm{dc}}+1}$ and $h_{\mathrm{dc}} = h_{\mathrm{dc}} + 1$
5: **until** $|\boldsymbol{\rho}^{h_{\mathrm{dc}}+1} - \boldsymbol{\rho}^{h_{\mathrm{dc}}}| \leq \epsilon_{\mathrm{dc}}$

$$\text{subject to } \sum_{j=1}^{J} e^{\rho_{n,j}} \leq p_{\max}, \forall n, j \qquad (29\mathrm{b})$$

$$I'_{\mathrm{SI}_j} \leq I_{\mathrm{req}_{j,l}}, \forall j, l, \qquad (29\mathrm{c})$$

$$f_k(\boldsymbol{\rho}) - h_k(\boldsymbol{\rho}) \geq R_{\mathrm{req}_k}, \forall k, \qquad (29\mathrm{d})$$

where $I'_{\mathrm{SI}_j} = \sum_{n=1}^{N} \sum_{k=1}^{K} \alpha_{n,j,k} e^{\rho_{n,j}} \|\mathbf{G}_{\mathrm{SI}_{n,j}}\|^2 / \delta_{\mathrm{SI}}$. It can be seen that the optimization problem in (29) becomes convex with the log-sum-exp function after employing DC scheme. Therefore, the problem can be solved after obtaining the approximation of $f_k(\boldsymbol{\rho})$ in the $\boldsymbol{\rho}$ domain via the sequential convex approximation using the first-order Taylor expansion as $f_k(\boldsymbol{\rho}) \approx f_k(\boldsymbol{\rho}^h) + \nabla f_k^{\mathrm{T}}(\boldsymbol{\rho}^h)(\boldsymbol{\rho} - \boldsymbol{\rho}^h)$, where $\boldsymbol{\rho}^h$ is the approximated solution at the h-th iteration, and $\nabla f_k(\boldsymbol{\rho}^h)$ is the gradient of $f_k(\boldsymbol{\rho})$ at $\boldsymbol{\rho}$ as $\nabla f_k(\boldsymbol{\rho}^h) = (\partial f_k(\boldsymbol{\rho}^h))/\partial \rho_{m,l})^{\mathrm{T}}, \forall m, l$. It should be noted that $\nabla f_k(\boldsymbol{\rho}^h)$ is a column vector with $N \cdot J$ elements. The (m, l)-th element of $\nabla f_k(\boldsymbol{\rho}^h)$ is given by $\frac{\partial f(\boldsymbol{\rho}^h)}{\partial \rho_{m,l}} = \frac{e^{\rho_{m,l}^h} \|\mathbf{g}_{m,l,k}\|^2}{\left(d'_{n,j,k} + I'_{t_{n,j,k}} + \sigma_{n,j,k}^2\right) \ln 2}$. By substituting $f_k(\boldsymbol{\rho}^h)$, $\nabla f_k^{\mathrm{T}}(\boldsymbol{\rho}^h)$ and $\frac{\partial f(\boldsymbol{\rho}^h)}{\partial \rho_{m,l}}$ into (29), the optimization problem can now be written as

$$\max_{\boldsymbol{\rho}} \sum_{k=1}^{K} R'_k \qquad (30\mathrm{a})$$

$$\text{subject to } (29\mathrm{b}) \text{ and } (29\mathrm{c})$$

$$\sum_{k=1}^{K} R'_k \geq R_{\mathrm{req}_k}, \forall k, \qquad (30\mathrm{b})$$

where $R'_k = f_k(\boldsymbol{\rho}^h) + \nabla f_k^{\mathrm{T}}(\boldsymbol{\rho}^h)(\boldsymbol{\rho} - \boldsymbol{\rho}^h) - h_k(\boldsymbol{\rho})$. Since R'_k is the addition of a linear ($\boldsymbol{\rho}$) and concave ($-h_k(\boldsymbol{\rho})$) functions, it can be seen that R'_k is a concave function with respect to the optimization variable $\boldsymbol{\rho}$, whereas (29b) and (29c) are convex functions. Thus, the problem in (30) can be solved by standard optimization tools, e.g., CVX. The proposed iterative DC algorithm for searching the solution of the problem in (30) is summarized in Algorithm 4.

D. Overall MCG-Based Resource Allocation Algorithm

The overall procedure of the proposed MCG algorithm is summarized in Algorithm 5 and is implemented in a repeated loop. After initialization of the basic parameters and PA decision $\mathbf{p}_{\mathrm{ini}}$, VA result $\mathbf{x}$ and initial RA policy $\boldsymbol{\alpha}_{\mathrm{mat}}$ are firstly obtained by Algorithms 1 and 2 (lines 1 to 3). An intermediate RA policy $\boldsymbol{\alpha}(i)$ and objective function value $\Theta_{\boldsymbol{\alpha}}(i)$ at i-th iteration are then attained and recorded by solving the RA sub-problem (17). Similarly, another intermediate PA decision $\mathbf{p}(i)$ and objective function value $\Theta_{\mathbf{p}}(i)$ are searched by

---

Algorithm 5 Proposed MCG Algorithm

1: Initialization:
    1) Set iteration index i, the maximum number of iterations $n_{\max}$, convergence threshold ϵ
    2) Initialize PA decision $\mathbf{p}_{\mathrm{ini}}$
2: Solve the (16) by Algorithms 1 and 2
3: Obtain $\mathbf{x}$ and $\boldsymbol{\alpha}_{\mathrm{mat}}$
4: **repeat**
5:     Solve the (16) by Algorithm 3 based on $\mathbf{x}$, $\mathbf{p}_{\mathrm{ini}}/\mathbf{p}(i-1)$ and $\boldsymbol{\alpha}_{\mathrm{mat}}/\boldsymbol{\alpha}(i-1)$
6:     Obtain $\boldsymbol{\alpha}(i)$ and $\Theta_{\boldsymbol{\alpha}}(i)$
7:     Solve (28) by Algorithm 4 based on $\boldsymbol{\alpha}(i)$
8:     Obtain $\mathbf{p}(i)$ and $\Theta_{\mathbf{p}}(i)$
9:     **if** $|\Theta_{\boldsymbol{\alpha}}(i) - \Theta_{\mathbf{p}}(i)| \leq \epsilon$ **then**
10:        **return** $\{\boldsymbol{\Pi}(i)\} = \{\boldsymbol{\alpha}(i), \mathbf{p}(i)\}$
11:    **else**
12:        $i = i + 1$
13:    **end if**
14: **until** $i = n_{\max}$

---

solving the PA sub-problem (30) via the standard CVX tool in Algorithm 4 (lines 4 to 8). The algorithm stops when the difference between $\Theta_{\boldsymbol{\alpha}}(i)$ and $\Theta_{\mathbf{p}}(i)$ at the i-th iteration is smaller than a predefined convergence threshold $\epsilon > 0$ or when the maximum iteration number $n_{\max}$ is reached (lines 9 to 14). Note that Algorithm 3 solves the RA sub-problem (17) based mainly on $\mathbf{p}(i-1)$ and $\boldsymbol{\alpha}(i-1)$, the value of $\mathbf{p}_{\mathrm{ini}}$ and $\boldsymbol{\alpha}_{\mathrm{mat}}$ are only adopted at the first iteration (line 5). In addition, for the RA sub-problem, the termination condition of Algorithm 1 ensures that at least one matched SBS of a given VUE can satisfy the QoS constraint.

IV. THEORETICAL ANALYSIS

In this section, the performance of the proposed MCG algorithm is analyzed in terms of various indicators. The analysis will be illustrated by discussing whether each sub-problem in the MCG method possesses the corresponding properties.

A. Effectiveness

Proposition 2: Total throughput of the considered network does not reduce after an iteration of the proposed MCG algorithm.

Proof: For the RA sub-problem, let $\boldsymbol{\Phi}$ and $\boldsymbol{\Phi}'$ represent the partitions obtained via Algorithm 3 after i and $(i+1)$-th dynamic operations, i.e., join, departure, replacement or switch, are implemented respectively. Then the difference of total ETR in the considered network between partitions $\boldsymbol{\Phi}'$ and $\boldsymbol{\Phi}$ can be written as

$$\Delta U_{\mathrm{r}}^{\mathrm{C}}(\boldsymbol{\Phi}', \boldsymbol{\Phi}) = \sum_{m=1}^{J} U_{\mathrm{r}}^{\mathrm{C}}(\Phi'_m) - U_{\mathrm{r}}^{\mathrm{C}}(\Phi_m), \qquad (31)$$

which can be calculated as

$$\Delta U_{\mathrm{r}}^{\mathrm{C}}(\boldsymbol{\Phi}', \boldsymbol{\Phi}) = \begin{cases} \sum_{p=j,j'} U_{\mathrm{r}}^{\mathrm{C}}(\Phi'_p) - U_{\mathrm{r}}^{\mathrm{C}}(\Phi_p), & \text{for SO,} \\ U_{\mathrm{r}}^{\mathrm{C}}(\Phi'_j) - U_{\mathrm{r}}^{\mathrm{C}}(\Phi_j), & \text{otherwise,} \end{cases} \qquad (32)$$

where j and j' are the indices of partitions that experience member variation when implementation of dynamic operations is completed, which have similar definitions as those in the discussions of Definitions 5 to 7. It should be noted that the number of partitions that undergoes member change in the SO is 2, while in the remaining operations is 1 from (32). After careful inspection of the CG algorithm, it can be concluded that $\Delta U_{\mathrm{r}}^{\mathrm{C}}(\mathbf{\Phi}', \mathbf{\Phi}) > 0$ from the conditions $U_{\mathrm{r}}^{\mathrm{C}}(\Phi'_j) + U_{\mathrm{r}}^{\mathrm{C}}(\Phi'_{j'}) > U_{\mathrm{r}}^{\mathrm{C}}(\Phi_j) + U_{\mathrm{r}}^{\mathrm{C}}(\Phi_{j'})$ and $U_{\mathrm{r}}^{\mathrm{C}}(\Phi'_j) > U_{\mathrm{r}}^{\mathrm{C}}(\Phi_j)$ in Definitions 5 to 7. For PA sub-problem, it can be seen that the objective function (29a) after i-th iteration can be expressed as

$$
\begin{aligned}
\sum_{k=1}^{K} & f_k(\boldsymbol{\rho}^i) - h_k(\boldsymbol{\rho}^i) \\
&= \sum_{k=1}^{K} f_k(\boldsymbol{\rho}^i) + \nabla f_k^{\mathrm{T}}(\boldsymbol{\rho}^i)(\boldsymbol{\rho}^i - \boldsymbol{\rho}^i) - h_k(\boldsymbol{\rho}^i) \\
&\overset{(a)}{\leq} \sum_{k=1}^{K} f_k(\boldsymbol{\rho}^i) + \nabla f_k^{\mathrm{T}}(\boldsymbol{\rho}^i)(\boldsymbol{\rho}^{i+1} - \boldsymbol{\rho}^i) - h_k(\boldsymbol{\rho}^{i+1}) \\
&\overset{(b)}{\leq} \sum_{k=1}^{K} f_k(\boldsymbol{\rho}^{i+1}) - h_k(\boldsymbol{\rho}^{i+1}),
\end{aligned} \tag{33}
$$

where the inequality (a) comes from the fact that $\boldsymbol{\rho}^{i+1}$ is the optimal solution of the PA sub-problem at i-th iteration. Inequality (b) results from the convexity of $f_k(\boldsymbol{\rho})$. To be more specific, for any given $\boldsymbol{\rho}$ and convex function $f_k(\boldsymbol{\rho})$, the following inequality will hold: $f_k(\boldsymbol{\rho}) \geq f_k(\boldsymbol{\rho}^i) + \nabla f_k^{\mathrm{T}}(\boldsymbol{\rho}^i)(\boldsymbol{\rho} - \boldsymbol{\rho}^i)$. The proof is therefore completed by the inequalities $\Delta U_{\mathrm{r}}^{\mathrm{C}}(\mathbf{\Phi}', \mathbf{\Phi}) > 0$ and (33). ■

B. Convergence

Proposition 3: Starting from any initial coalitional structure $\mathbf{\Phi}_{\mathrm{ini}}$ and PA policy $\mathbf{p}_{\mathrm{ini}}$, the proposed MCG algorithm converges after a finite number of iterations.

Proof: By Proposition 2, the throughput of the proposed method is improved after each iteration, which implies $R_{\mathrm{n}-1} \leq R_{\mathrm{n}}$, where R_{n} is the throughput after the n-th iteration of the proposed scheme. Moreover, since the amount of radio resource is limited, there exists a finite value R_{conv} such that R_{n} converges to R_{conv} when n is sufficiently large, which completes the proof. ■

C. Stability

The stability of the proposed MCG algorithm is studied by using the following definition.

Definition 8 (Nash-Stability) [28]: A coalition partition $\mathbf{\Phi} = \{\Phi_1, \cdots, \Phi_j\}$ is Nash-stable if $\forall k \in \mathcal{K}$, $U_{\mathrm{r}}^{\mathrm{C}}(\Phi_j) > U_{\mathrm{r}}^{\mathrm{C}}(\Phi_j \setminus k)$ and $U_{\mathrm{r}}^{\mathrm{C}}(\Phi_j) > U_{\mathrm{r}}^{\mathrm{C}}(\Phi_{j'} \cup k)$ for all $\Phi_j, \Phi_{j'} \subset \mathbf{\Phi}, k \in \Phi_j$, and $k \notin \Phi_{j'}$, which indicates that there is no incentive for a given VUE to either join or depart from a coalition.

Proposition 4: Given a fixed PA decision $\mathbf{p}$, the final partition $\mathbf{\Phi}^*$ obtained by Algorithm 3 for the RA sub-problem is Nash-stable.

Proof: The Nash-stability of the partition $\mathbf{\Phi}^*$ attained by Algorithm 3 can be proved by contradiction. Assuming

that the final partition $\mathbf{\Phi}^*$ searched by Algorithm 3 is not Nash-stable. Then, there exists a pair of coalitions Φ_j and Φ'_j and a VUE k such that $k \in \Phi_j$, and $k \notin \Phi'_j$ with inequalities $U_{\mathrm{r}}^{\mathrm{C}}(\Phi_j) < U_{\mathrm{r}}^{\mathrm{C}}(\Phi_j \setminus k)$ or $U_{\mathrm{r}}^{\mathrm{C}}(\Phi_j) < U_{\mathrm{r}}^{\mathrm{C}}(\Phi_{j'} \cup k)$ satisfied. Based on the principle of the proposed Algorithm 3, a dynamic operation will be performed to achieve better utility for the coalitions in the considered network, which contradicts the fact that $\mathbf{\Phi}^*$ is the final partition. Hence, we have completed the proof that final partition $\mathbf{\Phi}^*$ from the proposed Algorithm 3 is Nash-stable. ■

D. Optimality

The optimality of proposed MCG method is depicted based on the following definition.

Definition 8 (Stationary Point) [34]: Considering the following optimization problem

$$
\max_{\boldsymbol{\rho}} \ R(\boldsymbol{\rho}) \tag{34a}
$$

$$
\text{subject to } \boldsymbol{\rho} \in \mathcal{P}, \tag{34b}
$$

where $R(\boldsymbol{\rho})$ is a continuously differentiable function defined over the closed and convex set $\mathcal{P}$. Then $\boldsymbol{\rho}^* \in \mathcal{P}$ is called the stationary point of problem (34) if the following inequality is satisfied [35]: $\nabla R^{\mathrm{T}}(\boldsymbol{\rho}^*)(\boldsymbol{\rho} - \boldsymbol{\rho}^*) \leq 0$, for any $\boldsymbol{\rho} \in \mathcal{P}$. By using the inequality, the local optimality of the MCG algorithm is provided in the following proposition.

Proposition 5: Given a fixed RA policy $\boldsymbol{\alpha}$, the final PA decision $\mathbf{p}^*$ obtained by Algorithm 4 for the PA sub-problem can always reach the stationary point of problem (29), i.e., equation (25).

Proof: The objective function of PA sub-problem (30) can be rewritten as $R(\boldsymbol{\rho}) = \sum_{k=1}^{K} f_k(\boldsymbol{\rho}^i) + \nabla f_k^{\mathrm{T}}(\boldsymbol{\rho})(\boldsymbol{\rho} - \boldsymbol{\rho}^i) - h_k(\boldsymbol{\rho})$, where $\boldsymbol{\rho}^i$ is the obtained PA decision after i-th iteration. From the effectiveness and convergence properties described in Propositions 2 and 3 respectively, it can be seen that the obtained solution $\boldsymbol{\rho}^i$ when Algorithm 4 is convergent is the stationary point of problem (30), which satisfies the inequality $\nabla R^{\mathrm{T}}(\boldsymbol{\rho}^i)(\boldsymbol{\rho} - \boldsymbol{\rho}^i) \leq 0$. Note that $\boldsymbol{\rho}^i = \boldsymbol{\rho}^{i+1} = \boldsymbol{\rho}^*$ when Algorithm 4 converges. The inequality $\nabla R^{\mathrm{T}}(\boldsymbol{\rho}^i)(\boldsymbol{\rho} - \boldsymbol{\rho}^i) \leq 0$ can be equivalently expressed as

$$
\nabla \left(\sum_{k=1}^{K} f_k(\boldsymbol{\rho}^i) - h_k(\boldsymbol{\rho}^i) \right) (\boldsymbol{\rho} - \boldsymbol{\rho}^i) \leq 0. \tag{35}
$$

The proof is completed by the fact that $\left(\sum_{k=1}^{K} f_k(\boldsymbol{\rho}^i) - h_k(\boldsymbol{\rho}^i) \right)$ is the objective function of (29). ■

E. Complexity

Proposition 6: Let $\mathrm{O}_{\mathrm{mcg}}$ denote the computational complexity of the proposed MCG scheme. Then, we have $\mathrm{O}_{\mathrm{mcg}} \leq \mathcal{O}\left(\omega_{\mathrm{mcg}} \left(\omega_{\mathrm{coa}} + (NKJ)^2 \right) \right)$, where $\mathcal{O}$ means that the complexity is proportional to ω_{mcg} and ω_{coa} are the iteration numbers of the repeat loops in Algorithms 3 (line 2) and 5 (line 4), respectively.

Proof: For RA sub-problem, the complexity of Algorithms 1 to 3 are dominated by steps that are related to

calculations and comparisons of utility functions, as well as assignment of RBs, which causes complexity $\omega_{\text{mat}} K^2 NJ + KNJ$, $\omega_{\text{va}} K^2 N + KN$, and ω_{coa} respectively. ω_{mat} and ω_{va} are parameters in Algorithms 1 and 2 respectively that have similar definitions as ω_{mcg} and ω_{coa}. For PA sub-problem, it has been proved in [36] that globally optimal solution for PA sub-problem (25) can be obtained by linear programming method after applying branch and bound technique with complexity $\mathcal{O}\left((NKJ)^2 (NJ + JK + K)\right)$, where NKJ and $(NJ + JK + K)$ represent the number of optimization variable and constraint respectively. By [37], the method with lower approximation of the objective function will possess computational complexity less than $\mathcal{O}\left((NKJ)^2\right)$. Consequently, it can be observed that the complexity of Algorithm 4 is less than $\mathcal{O}\left((NKJ)^2\right)$ since the objective function (30a) is the lower bound approximation of (14a) in the original problem from the inequality $f_k(\boldsymbol{\rho}) \geq f_k(\boldsymbol{\rho}^i) + \nabla f_k^{\text{T}}(\boldsymbol{\rho}^i)(\boldsymbol{\rho} - \boldsymbol{\rho}^i)$ for any convex function $f_k(\boldsymbol{\rho})$. Therefore, the upper bound of complexity for Algorithm 5 can be calculated as $\omega_{\text{mat}} K^2 NJ + KNJ + \omega_{\text{va}} K^2 N + KN + \omega_{\text{coa}} + KJ + (NKJ)^2 = \omega_{\text{coa}} + KJ + (NKJ)^2 + K^2 N (\omega_{\text{mat}} + \omega_{\text{va}} J) + KN(1 + J)$. With the aid of big O notation, the upper bound of O_{mcg} for the MCG scheme in the worst case is $\mathcal{O}\left(\omega_{\text{mcg}}\left(\omega_{\text{coa}} + (NKJ)^2\right)\right)$, which completest the proof. ∎

F. Convergence Rate

Proposition 7: The proposed MCG algorithm achieves linear convergence.

Proof: Let R_{n} represents the throughput after the n-th iteration of the proposed scheme. Based on the convergence property shown in Proposition 3, we have $R_{\text{n}} \rightarrow R_{\text{conv}}$ as $n \rightarrow \infty$. By using the effectiveness property proved in the Proposition 2, the following inequality can be obtained: $R_{\text{n}+1} \geq R_{\text{n}}$. This inequality implies that there exists $r \in (0, 1)$ such that $\frac{|R_{\text{n}+1} - R_{\text{conv}}|}{|R_{\text{n}} - R_{\text{conv}}|} \leq r$ when n is sufficiently large, which satisfies the property of linear convergence [38]. The proof is therefore completed. ∎

V. NUMERICAL RESULTS

In this section, we evaluate the performance of the proposed algorithm and verify our theoretical analysis conducted in the previous section. Considering IBFD based network with one WBH, $N = 5$ SBSs and $K = 8$ VUEs uniformly distributed within 300×300 m^2 service area. Each SBS has 50 RBs to implement data transmission with carrier frequency equal to 2 GHz and maximum transmit power $p_{\text{max}} = 26$ dBm. The bandwidth of a RB is 180 kHz. The number of RB that is assigned to each SBS for backhaul links is in proportion to the number of its served VUEs. The pathloss effect of $\mathbf{g}_{n,j,k}(t)$ in (1) can be written as $s_{n,k} = 10^{-\text{PL}_{\text{NLOS}}/10}$ where pathloss model for non-line-of-sight (NLOS) is $\text{PL}_{\text{NLOS}} = 145.4 + 37.5 \log_{10} \nu_{n,k}$. $\nu_{n,k}$ is the distance between the n-th SBS and k-th VUE (in km). Moreover, $L = 3$ MCSs are chosen from 32 MCSs in LTE and the parameters for MCS modes 1 to 3 are $(\xi_1, \zeta_1) = (5.521, 1.521)$, $(\xi_2, \zeta_2) = (8.013, 0.947)$ and $(\xi_3, \zeta_3) = (16.7, 0.635)$. VUE speed,
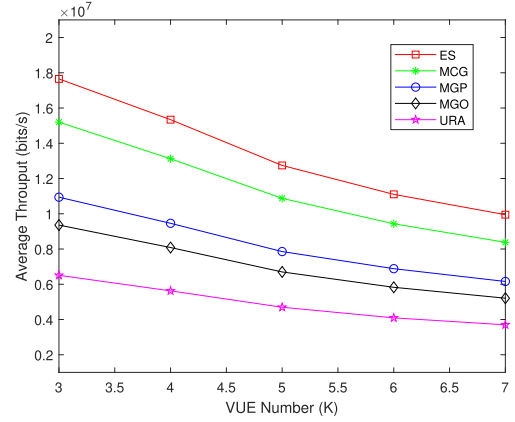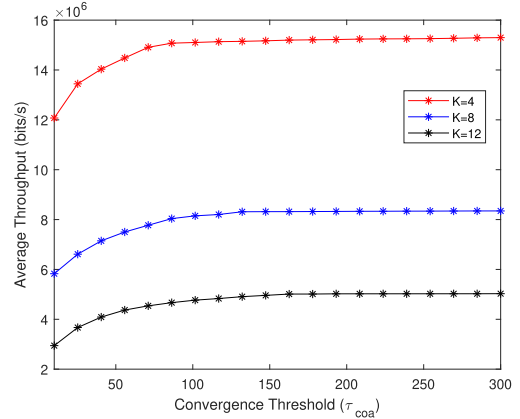

Fig. 2. Average throughput versus VUE number K.

Fig. 3. Average throughput versus convergence threshold τ_{coa} under different number of VUE.

reliability requirement B_{max}, latency requirement d_{req} and File size F_k are 50 km/h, 10^{-6}, 3 ms and 3000 bits, respectively. In addition, RB interference and SI cancellation amount are $\delta_{\text{r}} = 90$ dB and $\delta_{\text{SI}} = 85$ dB unless otherwise specified. These parameters are mainly referred from [1], [9], [16].

A. Performance of the Proposed Algorithm

The superiority of the proposed MCG algorithm is illustrated in Fig. 2 by showing average throughput versus the number of VUE K. For the purpose of performance comparison, four additional schemes are considered, which are described as follow.

(a) Exhaustive search (ES): The VA, RA and PA policies are determined after comparing all possible results, which can be considered as the performance upper bound.

(b) MG with PA (MGP) [22]: The VA and RA sub-problems are solved by MG and the solution for PA sub-problem are searched by applying variable transform technique as shown in (26).

(c) MG Only (MGO) [32]: MG is utilized to solve the VA and RA sub-problems whereas equal power allocation (EPA) is adopted for solving the PA sub-problem.

(d) Uniformly Random Allocation (URA): The VA and RA sub-problems are solved by allocating equal number of RB from a chosen SBS for each VUE in a random manner, while the solutions for PA sub-problem are obtained based on EPA.
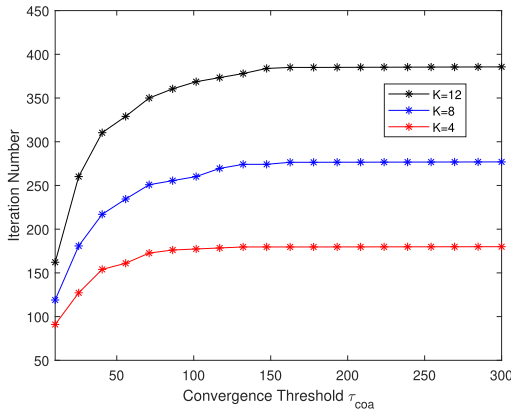
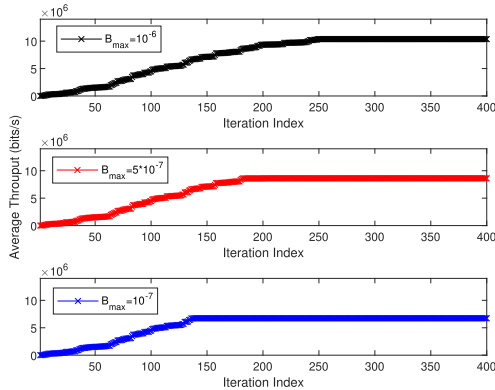Fig. 4. Iteration number versus convergence threshold τ_{coa} under different number of VUE.

Fig. 5. Average throughput versus iteration index under different reliability requirement B_{max}.

Fig. 6. Average throughput versus SI cancellation amount.

It can be seen that by combining CG with MG, the proposed MCG algorithm is able to achieve the smallest performance gap with the ES method, where the capacity gain comes from the cooperation among SBSs in the CG. The performance gain from the proposed MCG scheme is at least 15 % higher than the baseline schemes. In addition, compared with MGO, MGP method has higher average throughput since it benefits from additional PA. The URA scheme has the worst performance because both RB and power resources are randomly allocated. Moreover, due to the fact that the average amount of wireless resources assigned to each VUE is decreased as the number of VUE is increased, the average throughput is reduced when K becomes larger

The tradeoff between computational complexity and achievable performance of the proposed MCG algorithm under different number of VUE is illustrated in Figs. 3 and 4 by studying average throughput and iteration number versus convergence threshold τ_{coa}. Since larger convergence threshold τ_{coa} implies increased searching number and higher probability to obtain a pair of VUE and a coalition that will lead to implementation of dynamic operations, it is beneficial for the throughput improvement in the considered network. The average throughput is increased when τ_{coa} becomes larger at the price of larger iteration number. Moreover, as the proposed MCG method possesses the property of stability as illustrated in Proposition 4, both average throughput and iteration number become saturated when τ_{coa} is larger than 100. Furthermore, it is intuitive that the average amount of wireless resources
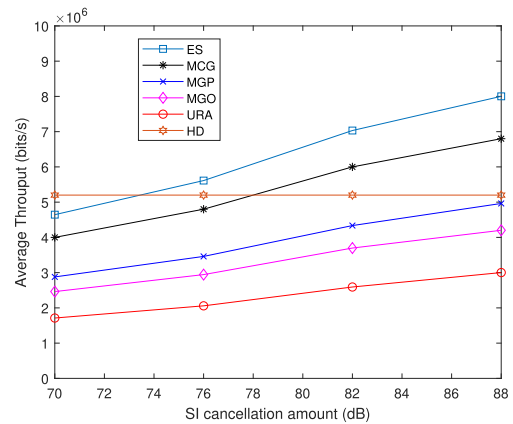
assigned to each VUE and the computational time to solve the considered optimization problem are decreased and increased respectively when the number of VUE is larger. Therefore, it can be seen from the figure that the average throughput when $K = 12$ is lower than that when $K = 4$ whereas the resulting iteration number is directly proportional to the VUEs' number. The effectiveness and convergence of the proposed MCG scheme when $\tau_{\text{coa}} = 100$ is investigated under different reliability requirement B_{max} in Fig. 5. It can be seen that the convergence of MCG method is achieved within 300 iterations while the average throughput is increased after each iteration at the same time. Hence, the properties of effectiveness and convergence in Propositions 2 and 3 are verified in this figure. Note that the convergence of the proposed method may induce additional computational delay and cause performance degradation in practical URLLC network. For instance, the solution has to be obtained when the number of iterations does not exceed 200 to satisfy the latency requirement of a URLLC network. In this case, the proposed algorithm is still highly applicable because the effectiveness property is beneficial for achieving maximal throughput within limited computational time. Moreover, recent literature in the field of hardware architecture has shown that the computational time for solving optimization problems can be significantly reduced [39]. Thus, the influence of computational delay can be mitigated by exerting the most up-to-date hardware technique. Moreover, since access links and backhaul links in the considered network use the same set of RBs, which implies that higher throughput in access links will cause larger SI power in backhaul links, the number of RBs that can be utilized in access links is limited by the reliability requirement B_{max} to guarantee the reliability in backhaul links. It can be observed that lower average throughput is obtained when B_{max} becomes more strict.

The performance comparison between half-duplex (HD) scheme with the proposed MCG scheme is shown in Fig. 6. Note that the average throughput of the HD scheme remains unchanged over all values of SI cancellation amount since it will not be affected by the SI. Moreover, the value of SI cancellation represents the SI power level, i.e., smaller SI cancellation amount implies stronger SI power and vice versa. It can be observed that the proposed scheme can remain
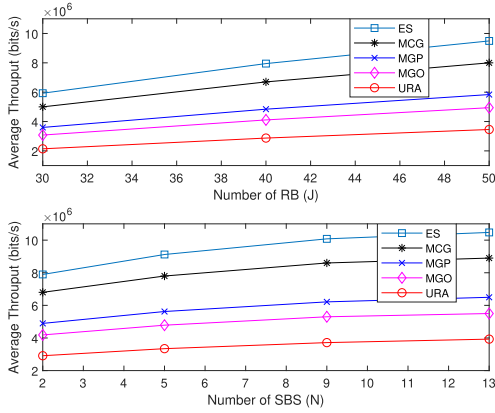
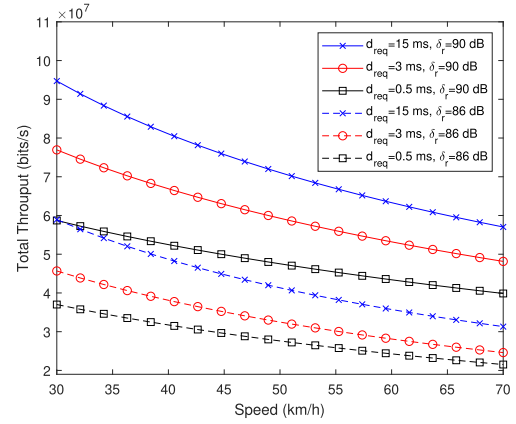Fig. 7. Average throughput versus RB number J and SBS number N.

Fig. 8. Total throughput versus VUEs' speed under different delay requirement d_{req} and RB interference cancellation capability δ_{r}.
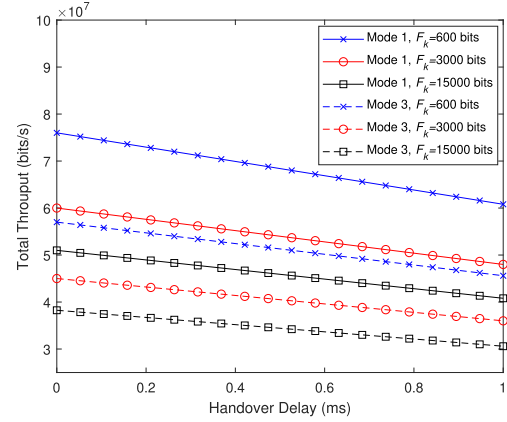

Fig. 9. Total throughput versus handover delay under different MCS scheme and file size F_k.

superior performance when SI cancellation amount is above 82 dB. Based on [40], current FD prototype can perform up to 120 dB SI cancellation amount. Hence, this figure shows that the proposed scheme can have better performance than HD scheme in practical scenarios.

The influence of different number of RB and SBS are shown in the top and bottom of Fig. 7, respectively. Since larger RB number implies that more radio resource can be used by VUEs in the networks, higher throughput is achieved when RB number is increased from the top of Fig. 7. Similar tendency can be observed in the bottom of Fig. 7. When SBS number is increased, VUE has higher probability to be associated with SBS that provides more radio resource. Hence, total throughput is improved when more SBS is deployed in the networks.

Note that Figs. 6 and 7 demonstrate consistent tendency with Fig. 2. Specifically, it can be seen that the proposed MCG scheme can achieve smallest performance gap with ES method since it provides additional opportunities to deviate from original matching result and find better solutions for VUEs. MGP outperforms MGO due to its more efficient PA, and URA has worst performance.

B. Impact of Mobility

In Fig. 8, the influence of VUEs' mobility is investigated by studying total throughput versus speed under different delay requirement d_{req} and RB interference cancellation capability δ_{r}. With increased VUEs' speed as seen from $\Delta S = S \cdot \frac{(v_k(t)f_cT_s)^2}{2v_c^2}$ in equations (5), the power of RB interference induced by Doppler shift is enlarged and leads to the decrement of total throughput. Moreover, different delay requirement implies the tradeoff between fairness and system performance. To be more specific, precious radio resources can be allocated to those VUEs with better channel condition when delay requirement is loose, whereas more wireless resources has to be assigned to VUEs with poor channel to satisfy latency constraint in (14c) when stringent delay requirement is imposed by VUEs. Hence, it can be observed that total throughput under delay requirement $d_{\mathrm{req}} = 15$ ms is higher than that when $d_{\mathrm{req}} = 3$ ms and 0.5 ms. Furthermore, since the power of RB interference can be suppressed to lower level, the considered network can reach higher total throughput when $\delta_{\mathrm{r}} = 90$ dB than $\delta_{\mathrm{r}} = 86$ dB, which suggests the importance

of RB interference cancellation capability in the considered network.

The effect of handover is depicted in Fig. 9 by studying total throughput versus handover delay under different MCS scheme and file size F_k. It can be seen that the establishment of a handover mechanism is necessary to ensure that handover delay does not affect the provision of URLLC service as total throughput will be decreased when handover delay becomes larger from $\eta_{n,k}(t)$ in (7). Moreover, since ξ_l and ζ_l are directly and inversely proportional to BLER respectively by $\mathrm{BLER}_{\mathrm{b}_j}(t) = \xi_l \exp(-\zeta_l \Gamma_{\mathrm{b}_j}(t))$ in (14b), the MCS scheme with lower index l is able to provide higher reliability and stronger robustness to SI power for backhaul links from the values of ξ_l and ζ_l. Hence, the network employing MCS mode 1 is allowed to use more RBs for access links before SI power constraint (16b) is violated and achieves higher total throughput than that utilizing MCS mode 3. Furthermore, due to the fact that larger file size F_k implies more rigorous data rate requirement from R_{req_k} in (16c) when delay requirement remains fixed, the total throughput when file size $F_k = 600$ bits is larger than those when $F_k = 3000$ bits and $F_k = 15000$ bits, which comes from the tradeoff between fairness and performance similar to Fig. 8.

C. Impact of SI Power

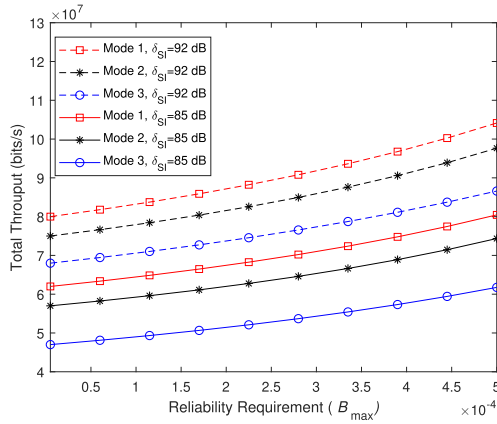The impact of SI power is illustrated in Fig. 10 by showing total throughput versus reliability requirement B_{max} under

Fig. 10. Total throughput versus reliability requirement B_{max} under different MCS mode and SI cancellation parameter δ_{SI}.

different MCS mode and SI cancellation capability δ_{SI}. Since $\ln(B_{max}) < 0$ when $B_{max} < 1$ by nature of the $\ln$ function, e.g., $\ln(B_{max}) = -2.3026$ and -4.6052 when $B_{max} = 10^{-1}$ and 10^{-2} respectively, it can be seen from $I_{req_{j,l}} = d_{b_j}(t) \cdot \left(-\frac{\zeta_l}{\ln(B_{max}/\xi_l)}\right) - \sigma_{b_j}^2$ in (16) that the larger value of the reliability requirement B_{max} results in the larger tolerable SI power $I_{req_{j,l}}$ so that more RBs can be utilized in access links. Thus, the total throughput of the considered network is increased when the reliability requirement B_{max} becomes larger. In addition, the influence of ξ_l and ζ_l on the total throughput can also be interpreted from the perspective of SI power. Specifically, the tolerable SI power $I_{req_{j,l}}$ is enlarged when the value of ξ_l and ζ_l are decreased and increased, respectively. Hence, the scenarios harnessing MCS mode with lower index l yield better total throughput. Moreover, because SI imposes stronger power when SI cancellation ability becomes weaker, a higher total throughput is obtained when $\delta_{SI} = 92$ dB compared with $\delta_{SI} = 85$ dB.

Note that as indicated in [41], in practical communications system and existing literatures, resource allocation, i.e., the assignment of channel resource and transmission power, are followed by adaptive selection of code rate and modulation schemes to match transmission parameters with time-varying channel conditions, which is an important aspect to enhance spectral efficiency. By adopting the model in (14b), the insight between the adopted MCS and tolerable SI power (which is reformulated from the reliability constraint) is provided in Fig. 10. Moreover, the insight between MCS and SI provided in Fig. 10 is beneficial for future design of adaptive MCS in networks with reliability constraint or SI. This important relationship cannot be obtained by adopting the normal approximation [26] method because it models error probability from information theory perspective but neglects MCS in the system. Hence, the model in (14b) is more advantageous to provide higher research insights from the resource allocation perspective.

VI. CONCLUSIONS

This paper studied the first resource management problem for the IBFD based V2I networks with guaranteed URLLC service. The considered problem includes the interference

in IBFD scheme along with handover delay and RB interference produced by VUEs' mobility that degrade system performance. With the design of novel handover delay model, the formulated resource allocation problem aimed to jointly optimize VA, RA and PA while satisfying the reliability and latency constraints in the meantime. To simplify the problem, an equivalent expression for the objective function is firstly derived. A MCG algorithm was then proposed after dividing the problem into two sub-problems. Theoretical analysis comprehensively investigates and demonstrates the properties of the proposed method. Simulation results verified the effectiveness of the theoretical results and illustrated the superiority of the proposed method when compared with the baseline schemes in the literatures.

REFERENCES

[1] J. Mei, K. Zheng, L. Zhao, Y. Teng, and X. Wang, "A latency and reliability guaranteed resource allocation scheme for LTE V2V communication systems," *IEEE Trans. Wireless Commun.*, vol. 17, no. 6, pp. 3850–3860, Jun. 2018.

[2] X. Ge, "Ultra-reliable low-latency communications in autonomous vehicular networks," *IEEE Trans. Veh. Technol.*, vol. 68, no. 5, pp. 5005–5016, May 2019.

[3] Z. Amjad, A. Sikora, B. Hilt, and J.-P. Lauffenburger, "Low latency V2X applications and network requirements: Performance evaluation," in *Proc. IEEE Intell. Vehicles Symp.*, Jun. 2018, pp. 220–225.

[4] A. A. Nasir, H. D. Tuan, H. H. Nguyen, M. Debbah, and H. V. Poor, "Resource allocation and beamforming design in the short blocklength regime for URLLC," *IEEE Trans. Wireless Commun.*, vol. 20, no. 2, pp. 1321–1335, Oct. 2020.

[5] S. He, Z. An, J. Zhu, J. Zhang, Y. Huang, and Y. Zhang, "Beamforming design for multiuser uRLLC with finite blocklength transmission," *IEEE Trans. Wireless Commun.*, vol. 20, no. 12, pp. 8096–8109, Dec. 2021.

[6] S. Samarakoon, M. Bennis, W. Saad, and M. Debbah, "Distributed federated learning for ultra-reliable low-latency vehicular communications," *IEEE Trans. Commun.*, vol. 68, no. 2, pp. 1146–1159, Nov. 2019.

[7] N. B. Khalifa, V. Angilella, M. Assaad, and M. Debbah, "Low-complexity channel allocation scheme for URLLC traffic," *IEEE Trans. Commun.*, vol. 69, no. 1, pp. 194–206, Jan. 2021.

[8] W. Wu, R. Liu, Q. Yang, H. Shan, and T. Q. S. Quek, "Learning-based robust resource allocation for ultra-reliable V2X communications," *IEEE Trans. Wireless Commun.*, vol. 20, no. 8, pp. 5199–5211, Aug. 2021.

[9] C. Guo, L. Liang, and G. Y. Li, "Resource allocation for low-latency vehicular communications: An effective capacity perspective," *IEEE J. Sel. Areas Commun.*, vol. 37, no. 4, pp. 905–917, Apr. 2019.

[10] M. Kamel, W. Hamouda, and A. Youssef, "Uplink coverage and capacity analysis of mMTC in ultra-dense networks," *IEEE Trans. Veh. Technol.*, vol. 69, no. 1, pp. 746–759, Jan. 2020.

[11] H. Ibrahim, H. ElSawy, U. T. Nguyen, and M.-S. Alouini, "Mobility-aware modeling and analysis of dense cellular networks with C-plane/ U-plane split architecture," *IEEE Trans. Commun.*, vol. 64, no. 11, pp. 4879–4894, Nov. 2016.

[12] H. S. Park, Y. Lee, T. J. Kim, B. C. Kim, and J. Y. Lee, "Handover mechanism in NR for ultra-reliable low-latency communications," *IEEE Netw.*, vol. 32, no. 2, pp. 41–47, Mar. 2018.

[13] U. Siddique, H. Tabassum, and E. Hossain, "Downlink spectrum allocation for in-band and out-band wireless backhauling of full-duplex small cells," *IEEE Trans. Commun.*, vol. 65, no. 8, pp. 3538–3554, Aug. 2017.

[14] Y. Li, P. Fan, L. Liu, and Y. Yi, "Distributed MIMO precoding for in-band full-duplex wireless backhaul in heterogeneous networks," *IEEE Trans. Veh. Technol.*, vol. 67, no. 3, pp. 2064–2076, Mar. 2018.

[15] L. Chen, F. R. Yu, H. Ji, G. Liu, and V. C. M. Leung, "Distributed virtual resource allocation in small-cell networks with full-duplex self-backhauls and virtualization," *IEEE Trans. Veh. Technol.*, vol. 65, no. 7, pp. 5410–5423, Jul. 2016.

[16] C.-H. Fang, P.-R. Li, and K.-T. Feng, "Joint interference cancellation and resource allocation for full-duplex cloud radio access networks," *IEEE Trans. Wireless Commun.*, vol. 18, no. 6, pp. 3019–3033, Jun. 2019.

[17] F. Yu, D. Li, Z. Wang, and Q. Guo, "Partial update sequential probabilistic integer least square inter carrier interference mitigation algorithm in mobile OFDM system," *IEEE Commun. Lett.*, vol. 20, no. 4, pp. 680–683, Apr. 2016.

[18] X. Ren, W. Chen, B. Gong, Q. Qin, and L. Gui, "Position-based interference elimination for high-mobility OFDM channel estimation in multicell systems," *IEEE Trans. Veh. Technol.*, vol. 66, no. 9, pp. 7986–8000, Sep. 2017.

[19] Z. Situ, I. W.-H. Ho, T. Wang, S. C. Liew, and S. C. Chau, "OFDM modulated PNC in V2X communications: An ICI-aware approach against CFOs and time-frequency-selective channels," *IEEE Access*, vol. 7, pp. 4880–4897, 2019.

[20] Z. Zhou, K. Ota, M. Dong, and C. Xu, "Energy-efficient matching for resource allocation in D2D enabled cellular networks," *IEEE Trans. Veh. Technol.*, vol. 66, no. 6, pp. 5256–5268, Jun. 2017.

[21] D. Wu, Q. Wu, Y. Xu, J. Jing, and Z. Qin, "QoE-based distributed multi-channel allocation in 5G heterogeneous cellular networks: A matching-coalitional game solution," *IEEE Access*, vol. 5, pp. 61–71, 2017.

[22] M. K. Elhattab, M. M. Elmesalawy, T. Ismail, H. H. Esmat, M. M. Abdelhakam, and H. Selmy, "A matching game for device association and resource allocation in heterogeneous cloud radio access networks," *IEEE Commun. Lett.*, vol. 22, no. 8, pp. 1664–1667, Aug. 2018.

[23] B. Zhang, X. Mao, and J.-L. Yu, "Resource allocation for 5G heterogeneous cloud radio access networks with D2D communication: A matching and coalition approach," *IEEE Trans. Veh. Technol.*, vol. 67, no. 7, pp. 5883–5894, Jul. 2018.

[24] G. Dong, H. Zhang, S. Jin, and D. Yuan, "Energy-efficiency-oriented joint user association and power allocation in distributed massive MIMO systems," *IEEE Trans. Veh. Technol.*, vol. 68, no. 6, pp. 5794–5808, Jun. 2019.

[25] Y. Zhao, X. Li, Y. Li, and H. Ji, "Resource allocation for high-speed railway downlink MIMO-OFDM system using quantum-behaved particle swarm optimization," in *Proc. IEEE Int. Conf. Commun. (ICC)*, Jun. 2013, pp. 2343–2347.

[26] Y. Polyanskiy, H. V. Poor, and S. Verdu, "Channel coding rate in the finite blocklength regime," *IEEE Trans. Inf. Theory*, vol. 56, no. 5, pp. 2307–2359, Apr. 2010.

[27] H. Zhang, H. Liu, J. Cheng, and V. C. M. Leung, "Downlink energy efficiency of power allocation and wireless backhaul bandwidth allocation in heterogeneous small cell networks," *IEEE Trans. Commun.*, vol. 66, no. 4, pp. 1705–1716, Apr. 2018.

[28] Y. Chen, B. Ai, Y. Niu, K. Guan, and Z. Han, "Resource allocation for device-to-device communications underlaying heterogeneous cellular networks using coalitional games," *IEEE Trans. Wireless Commun.*, vol. 17, no. 6, pp. 4163–4176, Jun. 2018.

[29] R. Ouyang, T. Matsumura, K. Mizutani, and H. Harada, "A robust channel estimation for IEEE 802.22 enabling wide area vehicular communication," in *Proc. 21st Int. Symp. Wireless Pers. Multimedia Commun. (WPMC)*, Nov. 2018, pp. 52–57.

[30] E. Ahmed and A. M. Eltawil, "All-digital self-interference cancellation technique for full-duplex systems," *IEEE Trans. Wireless Commun.*, vol. 14, no. 7, pp. 3519–3532, Jul. 2015.

[31] D. Nguyen, L.-N. Tran, P. Pirinen, and M. Latva-Aho, "On the spectral efficiency of full-duplex small cell wireless systems," *IEEE Trans. Wireless Commun.*, vol. 13, no. 9, pp. 4896–4910, Sep. 2014.

[32] S. Sekander, H. Tabassum, and E. Hossain, "Decoupled uplink-downlink user association in multi-tier full-duplex cellular networks: A two-sided matching game," *IEEE Trans. Mobile Comput.*, vol. 16, no. 10, pp. 2778–2791, Oct. 2017.

[33] Y. Li, D. Jin, J. Yuan, and Z. Han, "Coalitional games for resource allocation in the device-to-device uplink underlaying cellular networks," *IEEE Trans. Wireless Commun.*, vol. 13, no. 7, pp. 3965–3977, Jul. 2014.

[34] Y. Li, M. Sheng, C. Yang, and X. Wang, "Energy efficiency and spectral efficiency tradeoff in interference-limited wireless networks," *IEEE Commun. Lett.*, vol. 17, no. 10, pp. 1924–1927, Oct. 2013.

[35] S. Boyd and L. Vandenberghe, *Convex Optimization*. Cambridge, U.K.: Cambridge Univ. Press, Mar. 2004.

[36] J. Cui, Y. Liu, Z. Ding, P. Fan, and A. Nallanathan, "QoE-based resource allocation for multi-cell NOMA networks," *IEEE Trans. Wireless Commun.*, vol. 17, no. 9, pp. 6160–6176, Sep. 2018.

[37] W. Li, T. Chang, and C. Chi, "Multicell coordinated beamforming with rate outage constraint—Part II: Efficient approximation algorithms," *IEEE Trans. Signal Process.*, vol. 63, no. 11, pp. 2763–2778, Jun. 2015.

[38] J. Nocedal and S. J. Wright, *Numerical Optimization*, 2nd ed. New York, NY, USA: Springer, 2006.

[39] P. Vidal, E. Alba, and F. Luna, "Solving optimization problems using a hybrid systolic search on GPU plus CPU," *Soft Comput.*, vol. 21, no. 12, pp. 3227–3245, Jun. 2017.

[40] Z. Wei, X. Zhu, S. Sun, Y. Huang, A. Al-Tahmeesschi, and Y. Jiang, "Energy-efficiency of millimeter-wave full-duplex relaying systems: Challenges and solutions," *IEEE Access*, vol. 4, pp. 4848–4860, 2016.

[41] M. Mazzotti, S. Moretti, and M. Chiani, "Multiuser resource allocation with adaptive modulation and LDPC coding for heterogeneous traffic in OFDMA downlink," *IEEE Trans. Commun.*, vol. 60, no. 10, pp. 2915–2925, Oct. 2012.

Chun-Hao Fang (Student Member, IEEE) received the B.S. degree from the Department of Communications Engineering, National Chiao Tung University, Hsinchu, Taiwan, in 2014, and the Ph.D. degree from the Institute of Communications Engineering, National Chiao Tung University, in 2020. His research interests include interference cancellation, resource allocation design for full-duplex, cloud radio access networks, and 5G networks.

Kai-Ten Feng (Senior Member, IEEE) received the B.S. degree from the National Taiwan University, Taipei, Taiwan, in 1992, the M.S. degree from the University of Michigan, Ann Arbor, in 1996, and the Ph.D. degree from the University of California at Berkeley, Berkeley, in 2000.

He was with the Department of Electrical and Computer Engineering, National Yang Ming Chiao Tung University (NYCU), Hsinchu, Taiwan, as an Associate Professor and an Assistant Professor from August 2007 to July 2011 and February 2003 to July 2007, respectively, where he has been a Full Professor since August 2011. He has been serving as the Associate Dean for the Electrical and Computer Engineering College, NYCU, since February 2017. From July 2009 to March 2010, he was a Visiting Research Fellow with the Department of Electrical and Computer Engineering, University of California at Davis. Between 2000 and 2003, he was an In-Vehicle Development Manager/Senior Technologist with OnStar Corporation, a subsidiary of General Motors Corporation, where he worked on the design of future telematics platforms and in-vehicle networks. His current research interests include broadband wireless networks, cooperative and cognitive networks, smart phone and embedded system designs, wireless location technologies, and intelligent transportation systems. He received the Best Paper Award from the Spring 2006 IEEE Vehicular Technology Conference, which ranked his paper first among the 615 accepted papers. He also received the Outstanding Youth Electrical Engineer Award in 2007 from the Chinese Institute of Electrical Engineering and the Distinguished Researcher Award from NCTU in 2008, 2010, and 2011. He has served on the technical program committees in various international conferences. He has been serving as the Technical Advisor for the IEEE-HKN Honor Society and the National Academy of Engineering (NAE) Grand Challenges Scholars Program (GCSP) at NCTU since 2018.

Lie-Liang Yang (Fellow, IEEE) received the B.Eng. degree in communications engineering from Shanghai Tiedao University, Shanghai, China, in 1988, and the M.Eng. and Ph.D. degrees in communications and electronics from Beijing Jiaotong University, Beijing, China, in 1991 and 1997, respectively. From June 1997 to December 1997, he was a Visiting Scientist at the Institute of Radio Engineering and Electronics, Academy of Sciences of the Czech Republic. Since December 1997, he has been with the University of Southampton, U.K., where he is the Professor of wireless communications with the School of Electronics and Computer Science. He has published over 400 research papers in journals and conference proceedings, authored/coauthored three books, and also published several book chapters. He has research interests in wireless communications, wireless networks and signal processing for wireless communications, as well as molecular communications and nano-networks. He is a fellow of the IET and was a Distinguished Lecturer of the IEEE VTS. He served as an Associate Editor for the IEEE TRANSACTIONS ON VEHICULAR TECHNOLOGY and *Journal of Communications and Networks* (JCN), and is currently an Associate Editor of IEEE ACCESS and a Subject Editor of the *Electronics Letters*. The details about his research publications can be found at https://www.ecs.soton.ac.uk/people/llyang